Membrane-spanning lipids for an uncompromised monitoring of membrane fusion and intermembrane lipid transfer

Günter Schwarzmann,[1] Bernadette Breiden, and Konrad Sandhoff[1]

Life & Medical Sciences (LIMES) Institute, Membrane Biology & Lipid Biochemistry Unit, Kekulé-Institut für Organische Chemie und Biochemie, Universität Bonn, D-53121 Bonn, Germany

Abstract A Förster resonance energy transfer-based fusion and transfer assay was developed to study, in model membranes, protein-mediated membrane fusion and intermembrane lipid transfer of fluorescent sphingolipid analogs. For this assay, it became necessary to apply labeled reporter molecules that are resistant to spontaneous as well as protein-mediated intermembrane transfer. The novelty of this assay is the use of nonextractable fluorescent membrane-spanning bipolar lipids. Starting from the tetraether lipid caldarchaeol, we synthesized fluorescent analogs with fluorophores at both polar ends. In addition, we synthesized radioactive glycosylated caldarchaeols. These labeled lipids were shown to stretch through bilayer membranes rather than to loop within a single lipid layer of liposomes. More important, the membrane-spanning lipids (MSLs) in contrast to phosphoglycerides proved to be nonextractable by proteins. We could show that the GM2 activator protein (GM2AP) is promiscuous with respect to glycero- and sphingolipid transfer. Saposin (Sap) B also transferred sphingolipids albeit with kinetics different from GM2AP. In addition, we could unambiguously show that the recombinant activator protein Sap C x His_6 induced membrane fusion rather than intermembrane lipid transfer. These findings showed that these novel MSLs, in contrast with fluorescent phosphoglycerolipids, are well suited for an uncompromised monitoring of membrane fusion and intermembrane lipid transfer.—Schwarzmann, G., B. Breiden, and K. Sandhoff. **Membrane-spanning lipids for an uncompromised monitoring of membrane fusion and intermembrane lipid transfer. *J. Lipid Res.* 2015.** 56: **1861–1879.**

Supplementary key words chemical synthesis • fluorescence resonance energy transfer • glycolipids • lipid transfer proteins • *sn*-caldarchaeo-bis-phosphoethanolamine • *sn*-caldarchaeyl-bis-amine • 2-7-nitrobenz-2-oxa-1,3-diazol-4-yl-sphingolipids • labeled membrane-spanning lipids • glycosylated caldarchaeol

Protein-mediated membrane fusion and intermembrane lipid transfer are fundamental processes in many cellular functions and thus vital in cellular life. Fusion is important in the intracellular delivery of lipids, proteins, and metabolites by transport vesicles, endocytosis, exocytosis, cell division, and fertilization. Intermembrane lipid transfer has been found for all types of membrane lipids including glycolipids (1) and is especially essential in the degradative pathway of sphingolipids [for a review see (2, 3)]. Lysosomal lipid binding proteins such as the GM2 activator protein (GM2AP) and the four saposins Sap A, Sap B, Sap C, and Sap D, so-called cofactors or sphingolipid activator proteins (SAPs), are required for or assist in the enzymatic degradation of ganglioside GM1 (4) and GM2 (5–8), galactosylceramide (9), sulfatide (10), glucosylceramide (GlcCer) (11–13), and ceramide (Cer) (14, 15), respectively, by the appropriate lysosomal acid hydrolases. Some, if not all of these SAPs can act as lipid transfer proteins (LTPs) and facilitate extraction of lipids from biological membranes for their loading onto the lipid antigen-presenting CD1 molecules (16, 17). It has been

This work was supported by Grants SFB 645, SFB 284/B5, and the Special Program "Sphingolipids - Signals and Disease" (SA 257-24-2) funded by Deutsche Forschungsgemeinschaft (DFG).

Manuscript received 19 December 2014 and in revised form 22 July 2015.

Published, JLR Papers in Press, August 11, 2015
DOI 10.1194/jlr.M056929

Abbreviations: ATTO-MSPE, caldarchaeo-bis-*N*-ATTO647-phosphoethanolamine; BLC, bis-lactosyl-caldarchaeol and lactosyl-β-1,1[lactosyl-β-1′,1′]caldarchaeol; BMP, bis(monoacylglycero)phosphate; BSC, bis-sialyllactosyl-caldarchaeol and sialyllactosyl-β-1,1[sialyllactosyl-β-1′,1′] caldarchaeol; Cer, ceramide; DCM, dichloromethane; DOPC, dioleoyl glycerophosphocholine; DPPA, dipalmitoyl glycerophosphate; FRET, Förster resonance energy transfer; GlcCer, glucosylceramide; GM2AP, GM2 activator protein; LSC, lactosyl-sialyllactosyl-caldarchaeol and lactosyl-β-1,1[sialyllactosyl-β-1′,1′]caldarchaeol; LTP, lipid transfer protein; MSL, membrane-spanning lipid; MSPE, membrane-spanning phosphoethanolamine and sn-caldarchaeo-1,1′-bis-phosphoethanolamine; NBD, 7-nitrobenz-2-oxa-1,3-diazol-4-yl; NBDF, 7-nitrobenz-1,3-diazol-2-oxa-4-yl fluoride; NBD-MSL, caldarchaeyl-bis-*N*-NBD and 1,1′-didoxy-1,1′-bis-NBD-amino-caldarchaeol; NBD-MSPE, caldarchaeo-bis-*N*-NBD-phosphoethanolamine; NBD-PE, *N*-NBD-*sn*-1,2-dipalmitoylglycerophosphoethanolamine; Rh-PE, *N*-(lissamine rhodamine B sulfonyl)-*sn*-1,2-dipalmitoylglycerophosphoethanolamine; Sap, saposin; SAP, sphingolipid activator protein; SE, succinimidyl ester; TAMRA, 5-(and-6)-carboxytetramethylrhodaminyl; TAMRA-MSL, caldarchaeyl-bis-*N*-TAMRA and 1,1′-didoxy-1,1′-bis-TAMRA-amino-caldarchaeol; TAMRA-MSPE, caldarchaeo-bis-*N*-5-[and-6]-carboxytetramethylrhodaminyl-phosphoethanolamine; TCE, trichloroethylene; TDC, taurodeoxycholate; THF, tetrahydrofuran.

[1]To whom correspondence should be addressed.
e-mail: schwarzmann@uni-bonn.de (G.S.); sandhoff@uni-bonn.de (K.S.)

suggested that most of the SAPs act on lipids and sphingolipids of intraendolysosomal membranes. In vitro they bind to liposomal surfaces under acidic conditions, thus making membrane-bound sphingolipids available to their water-soluble exohydrolases (3, 8). For the study of membrane fusion and intermembrane lipid transfer, the use of liposomes as model biological membranes has become the method of choice. The procedures to detect fusion of lipid vesicles or intermembrane lipid transfer need to be not only sensitive but also reliable. Previously, Förster resonance energy transfer (FRET) (18) has been used to measure membrane fusion (19) as well as intermembrane lipid transfer (20, 21). A FRET assay allows us to measure in real time intermembrane lipid transfer and membrane fusion using model membrane systems (liposomes) without the need to separate liposomes. However, studies demonstrated that GM2AP transferred head group-labeled *sn* -1,2-diacylglycero phosphoethanolamine (22). Hence, these hitherto applied lipids are not well suited as membrane markers to study membrane fusion and protein-mediated intermembrane lipid transfer. To remedy this problem, one approach is to look for reporter lipids that could not be extracted from lipid bilayer membranes. It is well known that archaea (e.g., *Thermoplasma acidophilum*) thrive in the most extreme and arcane of environments with respect to heat and acidity. Even archaea lacking a cell wall can survive because they contain bipolar tetraether lipids that stabilize their plasma membrane. Owing to some indirect evidence such as the absence of a preferential fracture plane on the middle of a lipid bilayer (23–27) and on experiments of black lipid films of bipolar tetraether lipids (28–30), it is tacitly assumed that these bipolar tetraether lipids are membrane-spanning lipids (MSLs) and stretch across both leaflets of the plasma membrane of archaea. This fact suggested using labeled derivatives of bipolar lipids as reporter molecules for an improvement of the previously discussed membrane fusion and lipid transfer assays. A prerequisite for their use in the foregoing assays is that in model membranes, in which phosphoglycerolipids prevail, the labeled bipolar lipids almost exclusively stretch across the bilayer of liposomes rather than forming loops that would give them a U-shaped conformation as has been found for bipolar lipids on the air-water interface (31). For thermodynamic reasons, bipolar lipids in a stretched conformation, and hence membrane spanning, would not be vulnerable to extraction by proteins. We thus had to demonstrate that our newly synthesized caldarchaeol analogs do adopt a stretched conformation even at low concentration in lipid bilayers made of phosphoglycerolipids. Previously reported assays to evaluate the membrane activity of GM2AP include the transfer of radioactive GM2 between donor and acceptor vesicles (32, 33) and a fluorescence-dequenching assay based on the self-quenching of the lipid-probe octadecylrhodamine (34). Whereas the first method does not allow the continuous real-time monitoring of intermembrane lipid transfer and therefore impedes mechanistic studies, the latter system is not specific for ganglioside transfer activity and might not prove sensitive enough to reliably detect subtle differences in intermembrane transfer activity, for instance exhibited by GM2AP variants. To investigate the (glyco)sphingolipid binding and transfer activity of GM2AP and Saps, apart from their interaction with the respective enzyme, we had to develop a simple transfer assay that allowed rapid real-time measurement of membrane activity of GM2AP and Saps. This assay should yield unambiguous results and should be a significant improvement over the one published previously (20, 35). The aim of the present study was to improve a fast and simple FRET assay that allows an uncompromised monitoring in real time of intermembrane lipid transfer and membrane fusion using model membrane systems (liposomes) without the need to separate vesicles. We will demonstrate that labeled MSLs are well suited for this task.

MATERIALS AND METHODS

Materials

GM2AP from human kidney, Sap B from pig kidney, recombinant human Sap C x His_6, sialyllactose from cow colostrum, and 2-7-nitrobenz-2-oxa-1,3-diazol-4-yl (NBD)-sphingolipids were available in our laboratory. [^{3}H] sodium borohydride (spec. activity 370 TBq/mol) was obtained from PerkinElmer (Boston, MA), *N,N'*-dicyclohexylcarbodiimide, *N*-hydroxysuccinimide, 7-nitrobenz-1,3-diazol-2-oxa-4-yl fluoride (NBDF), and *N,N*-diisopropylethylamine were obtained from Fluka (Buchs, Switzerland). *N*-NBD-*sn*-1,2-dipalmitoylglycerophosphoethanolamine (NBD-PE), *N*-(lissamine rhodamine B sulfonyl)-*sn*-1,2-dipalmitoylglycerophosphoethanolamine (Rh-PE), and 5-(and-6)-carboxytetramethylrhodamine (TAMRA) succinimidyl ester (SE) (mixed isomers) was obtained from Molecular Probes (Eugene, OR). ATTO647N SE was obtained from ATTO-TEC (Siegen, Germany). LiChroprep RP-18, silica gel Si 60 (15–40 μm), prepacked silica gel chromatography columns Lobar type A, B, and C, TLC plates with fluorescence indicator (silica gel Si 60 F_{254}) were from Merck (Darmstadt, Germany). Dipalmitoyl glycerophosphate (DPPA), cholesterol, Dess-Martin periodinane (DMP), taurodeoxycholate (TDC), and neuraminidase (sialidase) from *Vibrio cholerae* were purchased from Sigma (Taufkirchen, Germany). Dioleoyl glycerophosphocholine (DOPC) and bis(monoacylglycero) phosphate (BMP) was from Avanti Polar Lipids (Alabaster, AL). All other reagents and chemicals used in this study were of the highest purity available.

Mass spectrometry

Mass spectra were recorded in positive ion mode on a Q-TOF 2 mass spectrometer (Micromass, Manchester, UK) equipped with a nanospray source. Analytes were dissolved in methanol or mixtures of methanol and benzene and were injected into the mass spectrometer by gold-coated glass capillaries (long type; Protana, Odense, Denmark) using a capillary voltage of 1,000 V and a cone voltage of 50 V at 80°C. Instrument calibration was done with a mixture of sodium iodide and cesium iodide in propanol-water (1:1, by volume). The MassLynx V 4.1 program (Waters, Milford, MA) was used for the deconvolution of the mass spectra.

Quantification of radioactivity

Radioactive compounds were quantified by scintillation counting using a Packard Tri-Carb 2900 TR liquid scintillation analyzer

(PerkinElmer, Rodgau, Germany). Radioactive compounds on TLC plates were analyzed using a phosphoimager (FUJIX BIO IMAGING ANALYZER IPR 1000; Fuji Photo Film Co. Ltd., Tokyo, Japan) and quantified by the program TINA V 2.09d (Raytest, Straubenhardt, Germany).

Cell culture

T. acidophilum [DSM 1728; German Collection of Microorganisms and Cell Cultures, Braunschweig, Germany] were cultivated similarly as described (36) under aerobic conditions at 59°C in 300 ml and 3 liter Erlenmeyer flasks containing 200 ml and 1.8 liter medium on a rotary shaker at 148 rpm (Infors, Bottmingen, Switzerland). The medium contained (per liter): 1.32 g $(NH_4)_2SO_4$, 0.372 g KH_2PO_4, 0.247 g $MgSO_4$ x 7 H_2O, 0.074 g $CaCl_2$ x 2 H_2O, 19.3 mg $FeCl_3$ x 6 H_2O, 1.8 mg $MnCl_2$ x 4 H_2O, 4.5 mg $Na_2B_4O_7$ x 10 H_2O, 0.22 mg $ZnSO_4$ x 7 H_2O, 0.05 mg $CuCl_2$ x 2 H_2O, 0.03 mg Na_2MoO_4 x 2 H_2O, 0.038 mg $VOSO_4$ x 5 H_2O, 0.02 mg $CoSO_4$ x 7 H_2O, 6 g yeast extract (Difco), and 10 g glucose. The pH was adjusted to 1.42 with 4 ml 50% H_2SO_4. To remove flocculants that appeared after a few hours standing at room temperature, this medium was filtered prior to use.

Cell growth was analyzed by measuring the optical density at 600 nm (Smart Spec 3000; Biorad, Hercules, CA). Archaea were harvested at an optical density $OD_{600\ nm}$ of 1.0 to 1.5 by centrifugation (6950 *g*, 5 min; Sorvall, Thermo, Germany). The cell pellets were washed several times with diluted sulfuric acid (1 ml sulfuric acid per liter water) until the supernatant remained clear and colorless after centrifugation. Finally, the pellets were washed acid free with water and stored at −80°C until use.

Lipid extraction and preparation of the core glyceryl di- and tetraether (i.e., archaeol and caldarchaeol)

Lipids from ~10 g frozen pellets containing archaea were extracted with chloroform-methanol (2:1, by volume) in a Soxleth device for 60 h under reflux. To cleave phosphoryl and glycosyl head groups, the evaporated total lipid fraction was methanolyzed in 1 M HCl in methanol for 36 h at 65°C (37). After evaporation of the solvent, the residue was dissolved in chloroform and washed twice with 10% Na_2CO_3 and three times with water. The chloroform fraction contained among many colored side products a small amount of the core glyceryl ethers [i.e., archaeol and caldarchaeol (dibiphytanyldiglycerol tetraether)]. Whereas archaeol was composed of a single species of diether lipid, caldarchaeol (including isocaldarchaeol) was a mixture of tetraether lipids containing from zero to six cyclopentane rings differing by only 2 mass units per ring and also containing the respective isocaldarchaeols (38, 39). Isocaldarchaeols and caldarchaeols with a parallel and antiparallel arrangement, respectively, of their glycerol moieties but otherwise isobaric could not be separated from each other under our purification condition. **Fig. 1A** shows an example of caldarchaeol with two cyclopentane rings and the stereochemistry as published (38, 40, 41). Under our culture conditions, caldarchaeols with one to three cyclopentane rings were predominant. The caldarchaeols were separated from archaeol and purified by repeated chromatography using prepared silica gel columns Lobar C and step gradients with mixtures of chloroform-ethyl acetate (from 9:1 to 1:1, by volume) as eluents. Fractions of caldarchaeols differing in their content of cyclopentane rings were obtained and characterized by ESI-quadrupole time-of-flight mass spectrometry. Caldarchaeols are easily ionized resulting in peaks $[M+H]^+$ at *m/z* 1,302.3, 1,300.3, 1,298.3, 1,296.3, and 1,294.3 for caldarchaeols with zero, one, two, three, and four five-membered rings, respectively. In the presence of ammonium acetate, the corresponding ions $[M+NH_4]^+$ were found at *m/z* 1,319.3, 1,317.3, 1,315.3, 1,313.3, and 1,311.3. For the synthesis of labeled bipolar lipids, we used fractions that contained mostly two cyclopentane rings (48%) besides one (26%) and three five-membered rings (22%) and ~4% of other caldarchaeols having none or four rings. Owing to the small mass difference of minus 2 mass units per additional cyclopentane ring, a complete separation into single species of caldarchaeol was difficult to achieve by our medium pressure chromatography and not pursued. For the purpose of our studies, this was also not necessary.

Caldarchaedial

The oxidation of a mixture of caldarchaeols (with mostly from one to three cyclopentane rings) was performed with DMP (42). Two hundred milligrams (470 μmol) solid periodinane was added to a solution of 300 mg (230 μmol) caldarchaeol in 2 ml dry dichloromethane (DCM) and 10 μl of tertiary butanol. The solid dissolved quickly by vigorous stirring and the reaction was complete after 45 min at 25°C. The resulting yellow turbid solution was centrifuged to remove deposits. Purification was by chromatography on silica gel in Lobar A with mixtures of chloroform-ethyl acetate (4:1, by volume). Besides ~30% mono-oxidation products, 200 mg of pure caldarchaedial was obtained in 66% yield with an Rf of ~0.9 on TLC in chloroform-ethyl acetate (4:1, by volume). The structure of the dialdehyde (Fig. 1A) was confirmed by mass spectrometry. Ions $[M+H]^+$ at *m/z* 1,296.3, 1,294.3, and 1,292.3 were found for caldarchaedial with one, two, and three cyclopentane rings when dissolved in methanol-benzene (1:1, by volume) shortly before measurement. When a solution of this dialdehyde was prepared in methanol with ammonium acetate, a classical chemical reaction of the carbonyl groups took place giving rise to semiacetals and semiaminals. In this case, ions $[M+2CH_3OH+NH_4]^+$ at *m/z* 1,377.3, 1,375.3, and 1,373.3 were most prominent besides ions $[M+2CH_3OH+NH_3-H_2O+H]^+$ at *m/z* 1,359.3, 1,357.3, and 1,355.3 for caldarchaedial with one, two, and three cyclopentane rings, respectively, in the lipid core.

Tritiated caldarchaeol

To ~100 mg (77 μmol) caldarchaedial in 500 μl 2-propanol/tetrahydrofuran (THF) (1:1, by volume) was added 0.76 mg (20 μmol) solid sodium borohydride at 10°C followed by 3.7 GBq solid sodium borotritiide. The solution was shaken at 10°C for 24 h. Then 2 mg of solid sodium borohydride was added, and shaking was continued for 12 h at 23°C. The reaction proved to be complete as checked by TLC in chloroform-ethyl acetate (4:1, by volume). Besides radioactive caldarchaeol (Rf ~0.4), some more polar radioactive side products of unknown nature had formed. Purification of tritiated caldarchaeol was by chromatography on silica gel in Lobar B with mixtures of chloroform-ethyl acetate (4:1 to 1:1, by volume). Approximately 68 mg of pure tritiated caldarchaeol with a specific radioactivity of 30 TBq (800 Ci/mol) was obtained in 68% yield. Mass spectra showed ions $[M+NH_4]^+$ at *m/z* 1,317.3, 1,315.3, and 1,313.3 for tritiated caldarchaeol with one, two, and three cyclopentane rings, respectively. Less prominent were ions $[M+Na]^+$ at *m/z* 1,322.3, 1,320.3, and 1,318.3 for tritiated caldarchaeol with one, two, and three cyclopentane rings, respectively. Small peaks of the respective doubly charged ions $[M+2NH_4]^{2+}$ appeared at *m/z* 667.7, 666.7, and 665.7. The structure of tritiated caldarchaeol is shown in Fig. 1B.

Deca-*O*-acetyl-monosialolactose-sialoyl-II^2-lactone

Approximately 80 mg (125 μmol) sialyllactose was treated with acetic anhydride in pyridine with a catalytic amount of 4-dimethylaminopyridine at 60°C for 2 days following a procedure described previously (43). Solvents were removed azeotropically with toluene, and the remaining residue was chromatographed on silica gel in Lobar B with acetone-toluene (1:1, by volume).

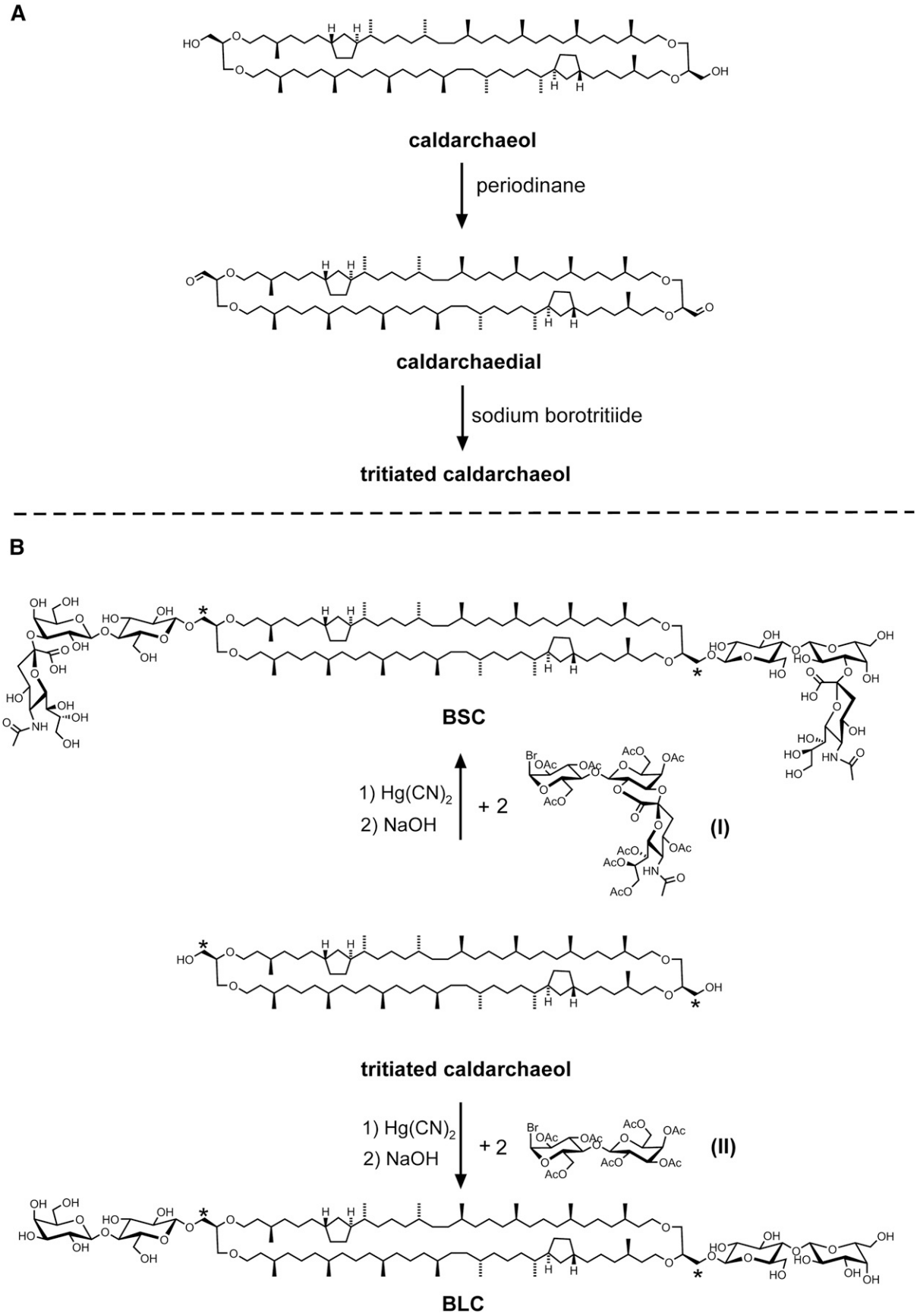

Fig. 1. A: Synthesis of tritiated caldarchaeol via its oxidation intermediate caldarchaedial. B: Synthetic route of radioactive sialyllactosyl-β-1,1[sialyllactosyl-β-1′,1′]caldarchaeol (BSC) and lactosyl-β-1,1[lactosyl-β-1′,1′]caldarchaeol (BLC) starting from tritiated caldarchaeol. Asterisks denote position of label.

Fractions with pure product were collected and freeze-dried from benzene to give 91 mg (88 μmol) deca-*O*-acetyl-monosialolactose-sialoyl-II^2-lactone in ~70% yield. TLC in acetone-toluene (1:1, by volume) showed one single spot with Rf of ~0.4. Further characterization was done by mass spectrometry. The mass spectrum was governed by ions $[M+NH_4]^+$ at *m/z* 1,053.3 and $[M+CH_3OH+NH_4]^+$ at *m/z* 1,085.3, demonstrating ring opening of some of the lactone molecules by methanol during sample preparation for mass spectrometry.

Nona-*O*-acetyl-α-monosialolactosyl bromide sialoyl-II^2-lactone (I)

The structure of the bromide I is shown in Fig. 1B and was prepared from deca-*O*-acetyl-monosialolactose-sialoyl-II^2-lactone essentially as described for tetradeca-*O*-acetyl-α-monosialogangliotetraosyl bromide sialoyl-II^2-lactone (43). Briefly, under ice cooling 65 mg deca-*O*-acetyl-monosialolactose-sialoyl-II^2-lactone was dissolved in 0.8 ml 30% HBr in glacial acetic acid and 8 μl acetic anhydride. After 30 min, the temperature was raised slowly to 20°C and kept for another 30 min. After the addition of 5 ml chloroform, the reaction mixture was extracted three times with 2 ml ice-cold water and 2 ml 0.1 M $NaHCO_3$. The organic phase was dried with sodium sulfate, taken to dryness under argon and finally freeze-dried from benzene. Sixty-four milligrams of I was obtained in better than 95% yield. The product produced one single spot on TLC in acetone-toluene (1:1, by volume), migrated slightly ahead of deca-*O*-acetyl-monosialolactose-sialoyl-II^2-lactone, and was used in the next synthetic step without further purification. Characterization was performed by mass spectrometry. The mass spectrum was governed by ions $[M+NH_4]^+$ at *m/z* 1,073.2 and 1,075.2, reflecting the two isomers of bromine. Lactone ring opening by methanol during sample preparation had also occurred yielding ions $[M+CH_3OH+NH_4]^+$ at *m/z* 1,105.3 and 1,107.3 for the two bromine isotopes.

Glycosylation of radioactive caldarchaeols

BSC. For the glycosylation of caldarchaeol, the long-known procedure of Koenigs and Knorr (44) as improved by Helferich and Weis (45) was followed with slight modification (46). Briefly, a solution of the α-bromide I (45 mg, 42 μmol) and 26 mg (20 μmol) radioactive caldarchaeol in 0.4 ml of a mixture of anhydrous toluene-nitromethane (1:4, by volume) was stirred in the presence of finely powdered anhydrous mercuric cyanide (30 mg) under argon in a screw-capped vial at 37°C for 24 h. During this period, radioactive caldarchaeol was completely converted into mainly three radioactive compounds as indicated by TLC in chloroform-ethyl acetate (1:1 by volume) with Rf of ~0.75, 0.1, and 0.0, respectively. Analysis by phosphoimaging showed that 55% of radioactivity was in the fast-moving compound, whereas 35% and 10% of radioactivity was in compounds with Rf of 0.1 and 0.0, respectively. The mixture was then diluted with 3 ml benzene and centrifuged to remove most of the salts. The supernatant was successively washed with water, 0.05 M sodium bicarbonate (2 × 2 ml), and water (2 × 2 ml); dried over sodium sulfate; and evaporated in a nitrogen stream. The residue was then purified by chromatography on silica gel in Lobar A using a stepwise elution with mixtures of chloroform-ethyl acetate (from 9:1 to 1:1, by volume) followed by chloroform-methanol (4:1, by volume). Radioactivity was followed by liquid scintillation counting. Three main radioactive fractions were collected, and their products were subjected to alkaline hydrolysis for 1 h at 60°C in a mixture of 1 ml methanol, 1 ml THF, and 0.4 ml 1 M NaOH. The hydrolyzed fast-moving compound turned out to be radioactive caldarchaeol (~50% of total radioactivity), that is, the radioactive starting material. Final purification of the saponified and combined two other products was by chromatography on silica gel in Lobar A using chloroform-methanol-water (65:25:4 followed by 60:35:8, by volume). Mono- and diglycosylation products (i.e., sialyllactosyl-β-1,1-caldarchaeol and BSC) were obtained in 25% and 8% yield of the starting radioactivity, respectively, and were characterized by mass spectrometry. For sialyllactosyl-β-1,1-caldarchaeol, prominent ions $[M+2NH_4]^{2+}$ were found at *m/z* 975.3, 974.3, and 973.3 for the monoglycosylation product with one, two, and three cyclopentane rings, respectively. Next in intensity were ions $[M+H+NH_4]^{2+}$ at *m/z* 966.8, 965.8, and 964.8 for the monosialyllactoside with one, two, and three cyclopentane rings, respectively. In addition, ions $[M+NH_4]^+$ were found at *m/z* 1,932.5, 1,930.5, and 1,928.5 for the monosialyllactoside with one, two, and three cyclopentane rings, respectively.

The mass spectrum of the bis-sialyllactoside BSC (Fig. 1B) confirmed its structure. The mass spectrum was governed by doubly charged ions $[M+2NH_4]^{2+}$ at *m/z* 1,282.8, 1,281.8, and 1,280.8 for BSC with one, two, and three cyclopentane rings, respectively. Further evidence of the structure was obtained by treating mixed micelles of BSC and TDC with neuraminidase (**Fig. 2B**, rightmost lane). A complete desialylation of BSC was obtained yielding a product that completely compared with synthetic BLC.

BLC. Using octa-*O*-acetyl-lactose as the starting sugar, BLC was synthesized from radioactive caldarchaeol via the bromide II (Fig. 1B) essentially as described for I and BSC. II was prepared and purified similarly as described for I. After de*O*-acetylation of the condensation product, BLC was purified and separated from a side product (i.e., lactosyl-β-1,1-caldarchaeol) by column chromatography using chloroform-methanol-water (65:25:4, by volume). Fractions with pure BLC showing one single spot on TLC [Rf ~0.4 and 0.56 when developed with chloroform-methanol-water (65:25:4 and 60:35:8, by volume, respectively)] were collected. Characterization was executed by mass spectrometry. Most prominent were ions $[M+2NH_4]^{2+}$ at *m/z* 991.8, 990.7, and 989.7 for BLC with one, two (Fig. 1B), and three cyclopentane rings, respectively. Ions $[M+NH_4]^+$ at *m/z* 1,965.5, 1,963.5, and 1,961.5 for BLC with one, two, and three cyclopentane rings were of less intensity.

Lactosyl-β-1,1[sialyllactosyl-β-1′,1′]caldarchaeol. For reference, a small amount of this monosialylated derivative was obtained by treating 500 μl liposomes with a total of 100 nmol lipids in 40 mM sodium acetate buffer pH 4.8 that contained 1 mM $CaCl_2$ with 50 mU of neuraminidase at 37°C. The liposomes were composed of 5 mol% of BSC besides 10 mol% DPPA, 10 mol% cholesterol, and 75 mol% DOPC. After 3 h, the reaction was stopped by adding 10 μl 2.5 M NH_3 and 5 min heating at 95°C. The solution was then dried under a nitrogen jet, and the residue was taken up in chloroform-methanol (1:1, by volume) and applied as a broad streak on a silica gel plate for preparative TLC chromatography using chloroform-methanol-water (60:35:8, by volume). The main radioactive band with Rf 0.35 was scraped from the plate, and material extracted from silica gel with chloroform-methanol (1:1, by volume). The characterization was by mass spectrometry. The ions $[M+2NH_4]^{2+}$ at *m/z* 1,137.3, 1,136.3, and 1,135.3 for lactosyl-β-1,1[sialyllactosyl-β-1′,1′]caldarchaeol (LSC) with one, two, and three cyclopentane rings, respectively, confirmed the structure of LSC, the monosialylated compound (Fig. 2A).

Synthesis of fluorescent caldarchaeols

sn-Caldarchaeo-1,1′-bis-phosphoethanolamine and membrane-spanning phosphoethanolamine (MSPE). The bis-phospho ethanolamine derivative of a purified caldarchaeol mixture containing mainly from one to three cyclopentane rings with a prevalence of those with two rings was prepared as outlined in **Fig. 3** with some modifications as described for the synthesis of phosphatidylethanolamine (47). Because the reaction is moisture sensitive, the reactants were

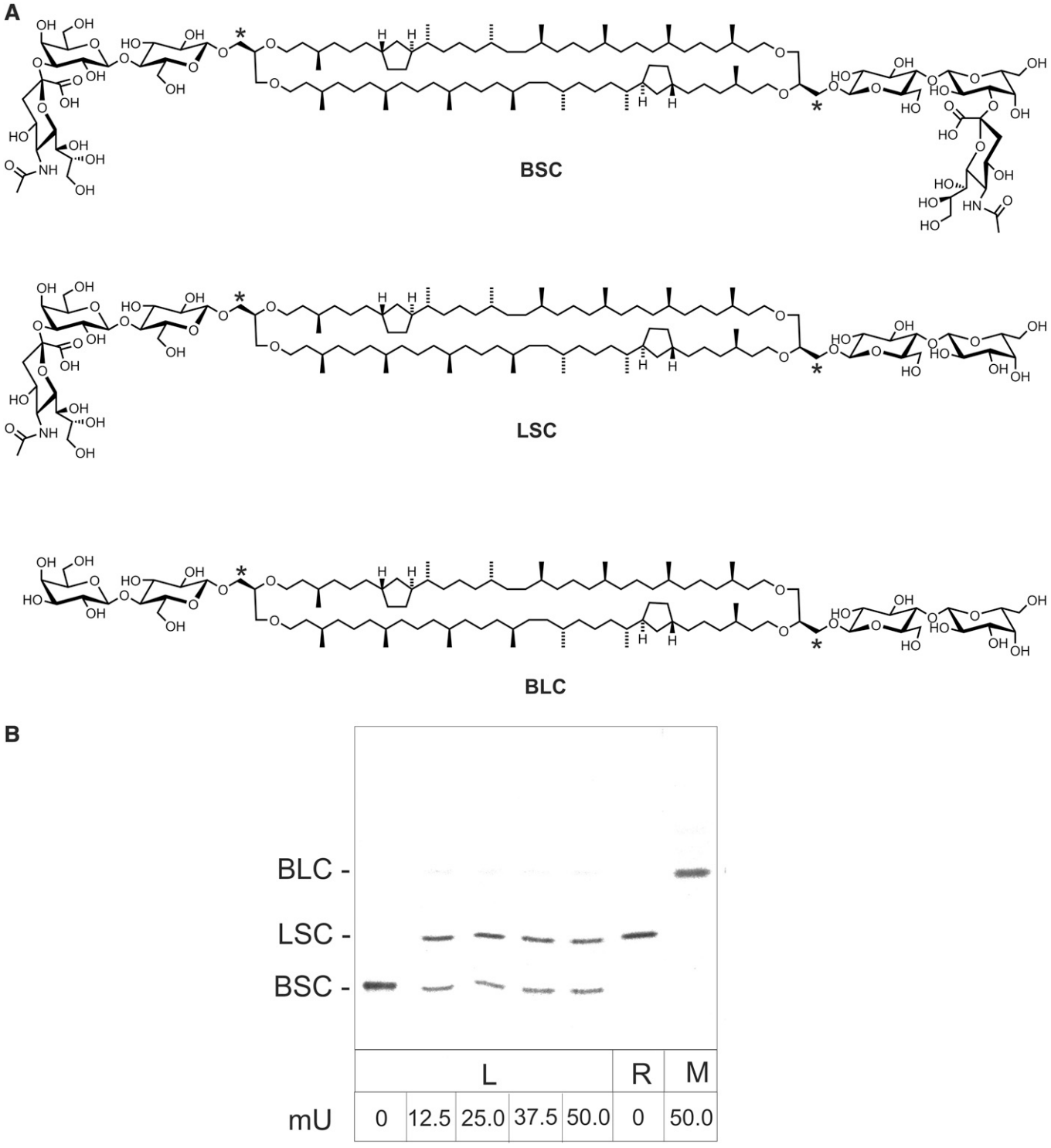

Fig. 2. Structure of synthetic bis-sialyllactosyl-caldarchaeol (BSC), lactosyl-sialyllactosyl-caldarchaeol (LSC), and bis-lactosyl-caldarchaeol (BLC) derived from tritiated caldarchaeol (A). Asterisks denote position of tritium label. To check whether caldarchaeol derivatives are stretched across the lipid bilayer, BSC-containing liposomes were incubated with varying amounts of neuraminidase (B). Second lane from right shows LSC used here for reference and obtained as described in Materials and Methods. The right-most lane depicts neuraminidase treatment of BSC in TDC micelles. Following neuraminidase treatment as described in Materials and Methods, the products were separated by TLC and visualized and quantified by phosphoimaging. All assays were carried out in triplicate, and the results agreed within 5%. L, liposomal assay; M, micellar assay; R, reference.

dissolved in freshly dried solvent and processed in reaction tubes that were cooled in a metal block with frequent droppings of liquid nitrogen to keep the temperature slightly below 5°C. Briefly, 75 µmol caldarchaeol having 150 µmol OH groups was dissolved in 600 µl trichloroethylene (TCE). This solution was taken up in a gas-tight syringe and slowly injected within 10 min via a needle pierced through the cap of an reaction tube into a precooled solution of 225 µmol phosphorus oxychloride dissolved

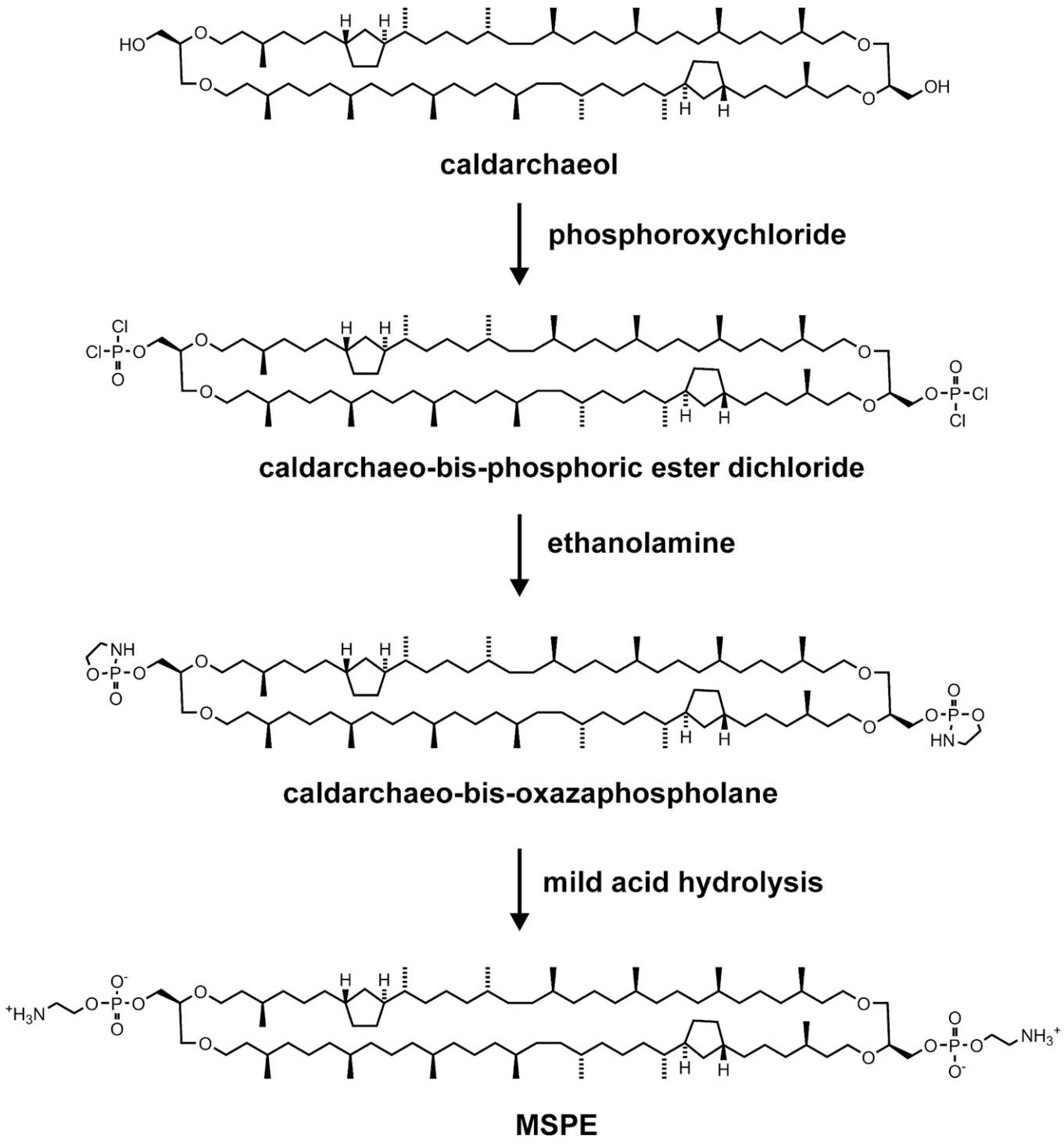

Fig. 3. Synthetic route to a membrane-spanning phosphoethanolamine (MSPE) derivative. Caldarchaeol was converted into caldarchaeo-bis-phosphoric ester dichloride using phosphoroxychloride in the presence of triethylamine. Treatment with ethanolamine produced caldarchaeo-bis-oxazaphospholane, which upon mild acid hydrolysis yielded MSPE as a precursor for membrane-spanning spacer-linked fluorophores (MSPE derivatives) as shown in Fig. 5A.

in a mixture of 75 μl n-hexane, 32 μl (225 μmol) triethylamine, and 150 μl TCE. Then the pierced hole was closed with self-adhesive tape. After further 10 min, the tube was centrifuged, and the resulting clear solution beneath the floating triethylammonium chloride was aspirated, diluted with 100 μl toluene, and then dried in an argon jet to remove solvents and the excess of phosphorus oxychloride. The oily residue representing caldarchaeo-bis-phosphoric acid ester dichloride was dissolved in 375 μl THF. To this solution was added dropwise a solution of 160 μmol ethanolamine and 600 μmol triethylamine in 375 μl THF at 10°C. Following centrifugation to sediment triethylammonium chloride the clear supernatant and two washings with THF were dried in an argon jet. The residue containing caldarchaeo-bis-oxazaphospholane was then dissolved in 500 μl THF,

300 µl methanol, and 200 µl 2-propanol. Mild acid hydrolysis was performed overnight after the addition of 500 µl of 40% acetic acid in water. A white precipitate had formed and was sedimented by centrifugation. The supernatant was dried and was redissolved together with the sediment in chloroform and methanol and then subjected to Folch partitioning (48). As revealed by TLC developed with chloroform-methanol-water (65:25:4, by volume), the lower phase contained MSPE (Rf 0.25) besides small amounts of side products such as MSPE methyl ester (Rf 0.52) and phosphoryl-caldarchaeo-phosphoethanolamine (Rf 0.13) and its methyl ester (Rf 0.30). For purification of the desired MSPE, the above mixture was first passed through a small column containing 4 ml of DEAE-Sephadex A 25 in the acetate form. The negatively charged lipids were retained on the column and could be eluted with a mixture of chloroform-methanol-water (3:7:1, by volume) containing 100 mM ammonium acetate. Nonretained MSPE, which had passed the column, was further purified by silica gel chromatography on Lobar A using chloroform-methanol-water (65:25:4, by volume). Fractions with purified MSPE were collected and characterized by mass spectrometry in the positive ion mode. Yield of colorless oily MSPE containing mostly from one to three cyclopentane rings was ~45%. For MSPE with two rings (Fig. 3), prominent ions $[M+H]^+$ were found at *m/z* 1,544.3 and 1,545.3. Ions at *m/z* 1,546.3 and 1,547.3, and 1,542.3 and 1,543.3 for MSPE with one and three cyclopentane rings, respectively, were also prominent in the mass spectrum. In addition, the corresponding ions $[M+2H]^{2+}$ were also found at *m/z* 772.6 and 773.1 for the compound with two rings as well as 773.6 and 774.1 for MSPE with one, and 771.6 and 772.1 for MSPE with three cyclopentane rings, respectively.

Preparation of caldarchaeyl-bis-tosylate. A solution of 108 mg (83 µmol) caldarchaeol in 1 ml benzene was dried under argon and then dissolved in 1.4 ml DCM. Following the addition of 70 µl triethylamine and 40 mg (209 µmol) tosylchloride, the reaction was complete after 4 h at 20°C. The organic phase was washed several times with 0.1 M sodium bicarbonate. Final purification was achieved by chromatography on silica gel in Lobar A using n-hexane-ethyl acetate (4:1, by volume) as eluent. One hundred thirty milligrams of pure caldarchaeol-bis-tosylate was obtained in 97% yield. The product gave one single spot on TLC (Rf 0.76) developed with n-hexane-ethyl acetate (7:3, by volume). Characterization was by mass spectrometry. Ions $[M+H]^+$ at *m/z* 1,608.3, 1,606.3, and 1,604.4 were obtained for the derivative with one, two (**Fig. 4**), and three cyclopentane rings in the lipid core, respectively. In the presence of ammonium acetate, the mass spectrum showed the respective ions $[M+NH_4]^+$ at *m/z* 1,625.3, 1,623.3, and 1,621.3.

Formation of caldarchaeyl-bis-azide. To a solution of 65 mg (40 µmol) caldarchaeol-bis-tosylate and 80 µmol 15-crown-5 (1,4,7,10,13-pentaoxacyclopentadecane) in 200 µl THF and 400 µl dimethylformamide was added 66 mg sodium azide. The mixture was stirred overnight at 50°C. Following addition of 6 ml DCM, the organic phase was washed several times with water to remove salts. After the organic solution was dried over sodium sulfate, final purification was achieved by column chromatography on silica gel using n-hexane-ethyl acetate (9:1, by volume). Fifty-two milligrams of pure caldarchaeol-bis-azide was obtained in 96% yield. TLC with n-hexane-ethyl acetate (9:1, by volume) revealed one single spot (Rf 0.7). The infrared spectrum displayed a characteristic band for azide oscillation at 2,090 cm^{-1}. Further characterization was done by mass spectrometry. Ions $[M+H]^+$ at *m/z* 1,350.3, 1,348.3, and 1,346.3 were obtained for the derivative with one, two, and three cyclopentane rings, respectively, in the lipid core. In the presence of ammonium acetate, the mass spectrum showed the respective ions $[M+NH_4]^+$ at *m/z* 1,367.3, 1,365.3, and 1,363.3. A side product was obtained in ~4% yield that according to mass spectrometry contained a tosyl group at one and an azido group at the other end; the respective ions $[M+NH_4]^+$ were found at *m/z* 1,496.3, 1,494.3, and 1,492.3 for this derivative with one, two, and three cyclopentane rings, respectively, in the core structure.

Caldarchaeyl-bis-amine. Caldarchaeol-bis-azide (5.4 mg, 4 µmol) was dissolved in a mixture of 200 µl n-hexane and 400 µl ethanol. After the addition of 3 mg PtO_2, hydrogenolysis was done overnight under 1 bar hydrogen pressure. The educt had disappeared, and finely dispersed platinum was removed by centrifugation. The supernatant was strongly basic owing to the generated amino groups. TLC in chloroform-methanol-water (65:25:4, by volume) showed one main spot (Rf 0.6). Yield was about 4.9 mg (3.8 µmol, 95%). This caldarchaeyl-bis-amine (Fig. 4) was used in the synthesis of fluorescent MSLs without further purification.

Caldarchaeo-bis-N-NBD-phosphoethanolamine. To a solution of 3.4 mg (2.2 µmol) MSPE in TCE/methanol (4:1, by volume) containing 10 µl diisopropylethylamine was added in increments of 20 µl a solution of NBDF (1.5 mg, 8.1 µmol) in 350 µl TCE/THF (3:1, by volume). The reaction was completed after 2 h at 20°C as checked by TLC. The crude product was purified by chromatography on silica gel in Lobar A using chloroform-methanol-water (65:25:4, by volume) as eluent. Fractions containing pure products, which on TLC in chloroform-methanol-water (65:25:4, by volume) showed only one fluorescent spot with Rf of ~0.28, were collected and characterized by mass spectrometry. The mass spectra showed prominent ions $[M+2NH_4]^{2+}$ at *m/z* 951.6, 952.6, and 953.6 for caldarchaeo-bis-*N*-NBD-phosphoethanolamine (NBD-MSPE) with three, two (**Fig. 5A**), and one cyclopentane ring, respectively. Total yield was 3.7 mg (1.96 µmol, 89%).

TAMRA-MSPE. A solution of 3.1 mg (2 µmol) MSPE in chloroform-methanol-water (65:25:4, by volume) was mixed with 30 µl diisopropylethylamine and 3.2 mg (6 µmol) solid TAMRA-SE. This SE dissolved after a few minutes, and the educt had disappeared after 6 h at 20°C as checked by TLC in chloroform-methanol-2 M NH_3 (60:35:8, by volume). A new dark red fluorescent compound with Rf of ~0.63 had appeared at the expense of MSPE (Rf ~0.51). This new compound was purified by chromatography on silica gel in Lobar A using chloroform-methanol-water (60:35:8, by volume) as eluent. Fractions that were free of the reagent and side products thereof were collected. Yield of pure TAMRA-MSPE was 2.9 mg (1.2 µmol, 60%). Characterization was by mass spectrometry. Ions $[M+2H]^{2+}$ at *m/z* 1,183.8, 1,184.8, 1,185.8, and 1,186.8 for TAMRA-MSPE with three, two, one, or zero cyclopentane rings, respectively, in the lipid core proved the structure of this compound (Fig. 5A). The respective triply charged ions $[M+3H]^{3+}$ at *m/z* 789.5, 790.2, 790.8, and 791.5 for TAMRA-MSPE with three, two, one, and zero cyclopentane rings, respectively, were also found in the mass spectrum. Furthermore, the respective ions $[M+2H+NH_4]^{3+}$ at *m/z* 795.3, 795.85, 796.5, and 797.2 were also present in the spectrum.

ATTO-MSPE. An ice-cold solution of ~1.6 mg (1 µmol) MSPE in chloroform-methanol-water (60:35:8, by volume) was mixed with 3 µl diisopropylethylamine and 3.1 mg (4 µmol) solid ATTO647N SE, which instantly dissolved. Reaction proceeded for 2 h at 20°C. TLC in chloroform-methanol-water (20:10:1, by volume) displayed a new dark blue compound with Rf of ~0.8 at

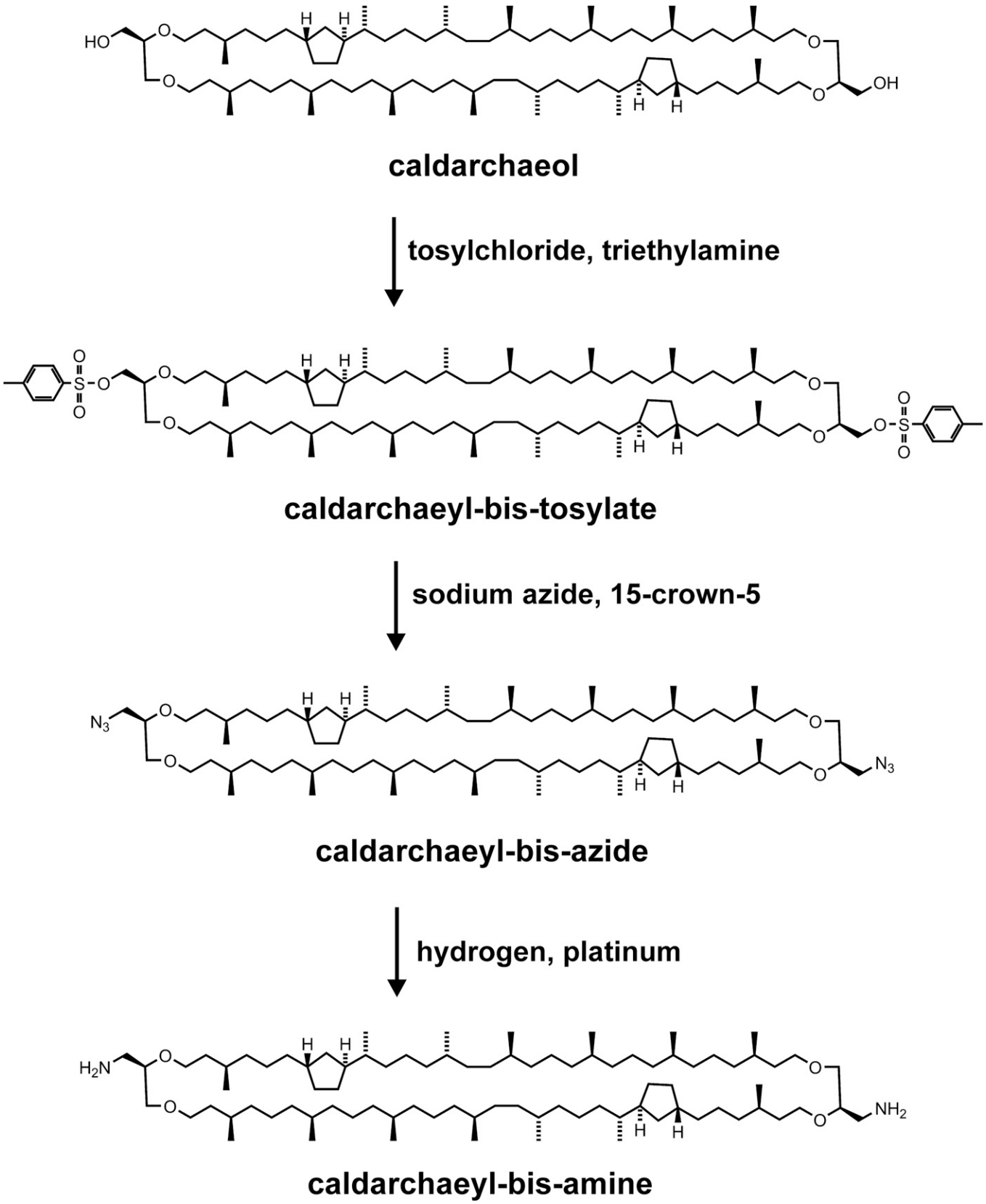

Fig. 4. Synthetic route to MSLs with fluorescent tags directly tied to the tetraether lipid core. Caldarchaeol reacted with tosyl chloride in the presence of triethylamine to give caldarchaeyl-bis-tosylate, which in the presence of the crown ether 15-crown-5 was transformed into caldarchaeyl-bis-azide. This azide was subjected to hydrogen in the presence of platinum to yield caldarchaeyl-bis-amine as a precursor for fluorescent MSL derivatives without a phosphoethanolamine spacer. So far a green and a red fluorescent derivative were obtained by reacting caldarchaeyl-bis-amine with amine-reactive fluorophores whose structures are shown in Fig. 5B.

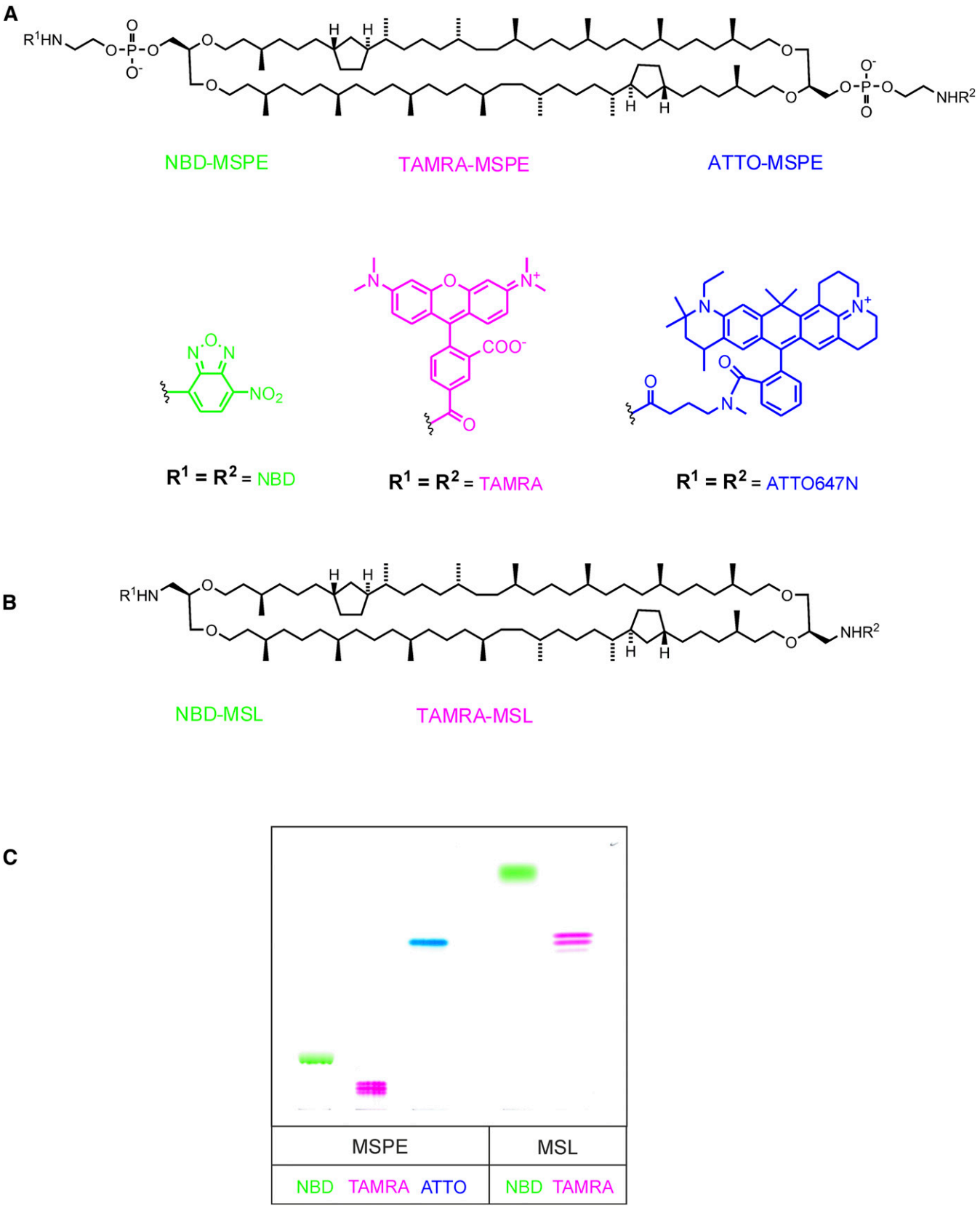

Fig. 5. Structures of homosubstituted MSPE (A) and MSL (B) derivatives with fluorescent tags linked via a phosphoethanolamine spacer (MSPE derivatives) or directly tied to the lipid core (MSL derivatives). C: A TLC plate of the respective fluorescent MSLs after development with chloroform-methanol-water (65:25:4, by volume). The plate was scanned normally with white light without special UV excitation. Except for NBD, the real compound's colors are shown. The NBD derivatives are yellow, but because this hue appeared too faint in the figure, a green color was chosen instead. ATTO-MSPE, caldarchaeo-bis-*N*-ATTO647-phosphoethanolamine; NBD-MSL, 1,1′-didoxy-1,1′-bis-NBD-amino-caldarchaeol; TAMRA-MSL, 1,1′-didoxy-1,1′-bis-TAMRA-amino-caldarchaeol; TAMRA-MSPE, caldarchaeo-bis-*N*-5-[and-6]-carboxytetramethylrhodaminyl-phosphoethanolamine.

the expense of MSPE. This new blue compound was purified by chromatography on silica gel in Lobar A using step gradient of chloroform-methanol-water (20:10:1 and 60:35:8, by volume) as eluent. Fractions that were free of side products were collected. Yield of pure ATTO-MSPE was 2 mg (0.75 μmol, 70%); its structure is shown in Fig. 5A. Characterization was by mass spectrometry. Ions $[M+2H]^{2+}$ at *m/z* 1,402.0, 1,401.0, 1,400.0, and 1,399.0 were characteristic for ATTO-MSPE with zero, one, two, and three cyclopentane rings in the lipid core, respectively. Even more pronounced were triply charged ions $[M+2H+NH_4]^{3+}$ at *m/z* 940.7, 940.0, and 939.3 for ATTO-MSPE with zero, one, and two cyclopentane rings, respectively. The respective ions $[M+3H]^{3+}$ at *m/z* 935.0, 934.3, and 933.7 are also prominent in the spectrum where the mass M is taken as the zwitterionic form with a formula weight of 2,798.1 for ATTO-MSPE with two five-membered rings in the lipid core.

Caldarchaeyl-bis-N-NBD. A solution of caldarchaeyl-bis-amine (~4 mg, 3 μmol) in 140 μl THF and 2 μl diisopropylethylamine was treated with 9 μmol (1.65 mg) NBDF at 20°C for 2 h. TLC in chloroform-methanol-1 M NH_3 (65:25:4, by volume) showed that the educt had disappeared and a new product had appeared at the front. A further TLC developed with n-hexane-ethyl acetate (7:3, by volume) showed a main product and a trace product with Rf of ~0.33 and 0.06, respectively, which by mass spectrometry in the presence of ammonium acetate turned out to be the bis-NBD and mono-NBD derivative, respectively. Final purification was achieved by column chromatography on silica gel with n-hexane-ethyl acetate (1:1, by volume). Fractions with pure compounds as checked by TLC were collected. Total yield was 3.3 mg (2 μmol, 67%). For caldarchaeyl-bis-*N*-NBD (NBD-MSL), prominent ions $[M+NH_4]^+$ were found at *m/z* 1,637.3, 1,639.3, and 1,641.3 for the bis-NBD derivative with three, two, and one cyclopentane rings, respectively. The structure is depicted in Fig. 5B.

Caldarchaeyl-bis-N-TAMRA. A solution of caldarchaeyl-bis-amine (~4 mg, 3 μmol) in 600 μl DCM/THF (1:1, by volume) and 5 μl diisopropylethylamine was treated with 10 μmol (5.2 mg) TAMRA-SE (5 and 6 isomers) at 30°C for 20 h. Thereafter, the reaction solution was diluted with 4 ml DCM and extracted four times with 3 ml water. The organic solution was dried over sodium sulfate, and the product purified on silica gel in Lobar A using chloroform-methanol-2 N NH_3 (65:25:4, by volume). On TLC in the same solvent system, purified caldarchaeyl-bis-*N*-TAMRA (TAMRA-MSL) separated into a double band with Rf of ~0.70 and 0.67 most likely due to the 5 and 6 isomer of the TAMRA residue. A further purification was not pursued and was not relevant for the use of this compound as a nonextractable and membrane-spanning energy quencher for an excited NBD fluorophore in bilayer membranes.

Yield of purified TAMRA-MSL containing besides mainly two also one and three cyclopentane rings in the lipid core was ~3.8 mg (1.8 μmol, 60%). Characterization was done by mass spectrometry. Prominent ions $[M+2H]^{2+}$ were found at *m/z* 1,059.7, 1,060.7, and 1,061.8 for TAMRA-MSL with three, two, or one cyclopentane ring, respectively. In addition, the respective ions $[M+H]^+$ were found at *m/z* 2,118.5, 2,120.5, and 2,122.5. The mass spectrum also showed small peaks for triply charged ions $[M+3H]^{3+}$ and $[M+2H+NH_4]^{3+}$. These mass spectra confirmed the structure of TAMRA-MSL (Fig. 5B).

Liposome preparation

For transfer and fusion assays, liposomes contained BMP, a lysosomal acidic phospholipid (49, 50). Donor vesicles for fusion assays were prepared with the following composition: 73 mol% DOPC, 5 mol% cholesterol, 20 mol% BMP, 1 mol% NBD-MSPE, and 1 mol% TAMRA-MSPE in a total of 200 nmol/ml 20 mM sodium citrate buffer pH 4.3 being 150 mM in NaCl. Donor liposomes for transfer assays were prepared with the following composition: 72 mol% DOPC, 5 mol% cholesterol, 20 mol% BMP, 2 mol% 2-NBD-(glyco)sphingolipid, and 1 mol% TAMRA-MSPE in a total of 200 nmol/ml 20 mM sodium citrate buffer pH 4.3 being 150 mM in NaCl. Acceptor vesicles consisted of 75 mol% DOPC, 5 mol% cholesterol, and 20 mol% BMP in a total of 1,000 nmol/ml 20 mM sodium citrate buffer (pH 4.3; 150 mM in NaCl). We have chosen this low pH value because of the fact that in lysosomes a low pH prevails and that the interaction of GM2 with GM2AP and β-hexosaminidase A is optimal in a narrow realm ~pH 4.3 (51, 52). For the liposome preparation, appropriate amounts of lipids from stock solutions were mixed and dried under nitrogen. The lipid mixture was then hydrated in citrate buffer (20 mM, pH 4.3), and this dispersion subjected to 10 freeze-thaw cycles. Large unilamellar vesicles were then prepared by extrusion 21 times through a polycarbonate filter with a pore size of 100 nm in a small extruder (LiposoFast; Avestin, Ottawa, ON, Canada). The filter used adsorbed a noticeable percentage of lipids. Therefore, every liposome preparation was done twice whereby the first extrusion process served to saturate the polycarbonate filter and was discarded. The liposome preparations used after the second extrusion process with the desired lipid composition contained in addition to unilamellar also some bilamellar vesicles as revealed by <50% reduction of the NBD group by dithionite (data not shown). Alternatively, liposomes could also be prepared by ultrasonication in a Branson sonifier cup horn (Branson, Danbury, CT). Although not always yielding liposomes as uniform in size as those gained by extrusion, the ultrasonication procedure was significantly more time and material saving.

FRET-based transfer assay

The final donor vesicle concentration in the assay mixture was 20 nmol lipid per ml, the concentration of acceptor vesicles 100 nmol lipid per ml in a total volume of 400 μl in 20 mM citrate buffer, pH 4.3 being 150 mM in NaCl. The transfer of *N*-NBD-PE, 2-NBD-GM2, 2-NBD-sulfatide, 2-NBD-GlcCer, or 2-NBD-Cer, respectively, was started by the addition of 0.25 μM GM2AP or 2.5 μM Sap B to the vesicle mixture. For the measurement of *N*-Rh-PE transfer, the donor liposomes contained ATTO-MSPE in place of TAMRA-MSPE as a quencher. Fluorescence measurements in a quartz cuvette were performed in a Shimadzu RF 5000 instrument (Kyoto, Japan) with an excitation wavelength of 468 nm and 540 nm for NBD lipids and Rh-PE, respectively. NBD and Rh emission was measured at 522 nm and 570 nm, respectively. A 100% dequench is defined by the fluorescence measured in the absence of quencher. Transfer was monitored at 28°C. Under our experimental conditions, photobleaching was negligible as for each time point the shutter was opened for 3–4 s only resulting in a total of 39–52 s of illumination. With continuous illumination, photobleaching over 1 h was linear with a loss of fluorescence of <0.3% fluorescence units per minute.

FRET-based fusion assay

For fusion assays, the concentrations of donor and acceptor vesicles and buffer were as for the transfer assays. In this case, however, donor liposomes contained 1 mol% of nonextractable NBD-MSPE in lieu of NBD-sphingolipids. Fusion was started by the addition of recombinant Sap C with a His_6-tag or with GM2AP or Sap B, respectively. Dequenching of the NBD fluorescence was measured at 522 nm as mentioned previously with an excitation wavelength of 468 nm. A 100% dequench is defined by the fluorescence measured in the absence of quencher.

Sialidase treatment of BSC

Sialidase (also called neuraminidase) treatment of BSC was performed in micelles of TDC as well as in model membranes. Mixed micelles composed of TDC (95 mol%) and BSC (5 mol%) were prepared in 20 mM sodium acetate pH 4.58 containing 0.5 mM $CaCl_2$. The micellar assay contained in a total of 50 µl 95 nmol TDC, 5 nmol BSC, and 1 nmol BSA. Following addition of 50 mU of neuraminidase the solution was gently shaken at 37°C for 60 min. Hydrolysis was then stopped by the addition of 10 µl 2.5 M NH_3 and 5 min heating at 95°C. The solution was then dried under a stream of nitrogen, and the residue taken up in chloroform-methanol (1:1, by volume) for TLC analysis and phosphoimaging.

Liposomes for the sialidase assay from a total of 200 nmol lipid were prepared in 1 ml 40 mM sodium acetate buffer (pH 4.8) and were composed of 5 mol% radioactive BSC besides 75 mol% DOPC, 10 mol% DPPA, and 10 mol% cholesterol. Following the addition of 12.5 to 50 mU of neuraminidase, these liposomes were treated as for the micelles as discussed previously. Analysis was by TLC and phosphoimaging.

RESULTS AND DISCUSSION

Demonstration that caldarchaeol derivatives are membrane spanning

For our approach of a FRET-based fusion and transfer assay, it became necessary to apply labeled reporter molecules that are resistant to spontaneous as well as protein-mediated intermembrane transfer. We have therefore prepared the lipid core of these tetraether lipids [i.e., caldarchaeols (including isocaldarchaeols)], from cultured *T. acidophilum* and used them for the synthesis of a variety of labeled reporter molecules. In Fig. 1A, the structure of caldarchaeol with two cyclopentane rings is shown. The nomenclature for derivatives of caldarchaeols used throughout this paper follows published recommendations (53, 54). The configuration of caldarchaeol as shown here was deduced previously mostly by chemical methods (24, 38, 40, 41, 55). As isocaldarchaeols and caldarchaeols just differ in a parallel versus antiparallel arrangement of their two glycerol moieties, respectively, it was not possible to separate them. Separation of these two species as well as complete fractionation into single species with respect to the number of cyclopentane rings was also not necessary for our preparation of nonextractable and labeled reporter molecules. Previously, evidence was presented that bipolar tetraether lipids span the entire membrane when arranged as a liposomal structure (25). We assumed that in bilayer model membranes, caldarchaeol derivatives, when present in only a small percentage, would also stretch across the entire bilayer rather than assuming a U-shaped conformation in a single lipid layer. This supposition called for a test. We therefore synthesized a tritium-labeled caldarchaeol and glycosylated both polar ends to obtain a BSC (Fig. 2A) and treated liposomes containing 5 mol% BSC with membrane-impermeable neuraminidase. If BSC spanned across the bilayer, the enzyme could split only the sialic acid residue facing the exoliposomal side. Fig. 2B depicts a representative TLC separation of products obtained after hydrolysis of BSC by increasing amounts of neuraminidase. The quantitative data indicate that BSC was mostly split into the monosialo compound LSC (76.5%) with very little complete desialylation to BLC (1.8%) confirming that most, if not all, BSC molecules span the bilayer. The fact that on average ~2% of BSC was completely hydrolyzed to BLC does not necessarily mean that few molecules of BSC adopt a U-shaped conformation in liposomal membranes. It is not unlikely that in the process of vesicle preparation a tiny percentage of lipid aggregates other than liposomes is formed such as, for example, micelles (56) and bicelles (57). If those aggregates were present, both ends of bipolar MSLs like BSC would be accessible to neuraminidase. This was confirmed by a total hydrolysis of BSC to BLC by neuraminidase when BSC was treated in TDC micelles (Fig. 2B, right-most lane). In liposomes, however, despite increasing amounts of neuraminidase, some of BSC (21.7%) remained unhydrolyzed possibly due to the presence of bilamellar membranes in our liposome preparation. This was supported by the observation that instead of 50% of NBD-MSPE only ~40% was reduced by dithionite (58) in liposomes prepared similarly (data not shown). The fact that with increasing amounts of the enzyme no LSC in liposomes was further hydrolyzed to BLC strongly indicates that the bipolar tetraether lipids span the phosphoglycerolipid bilayer rather than assuming a U-shaped conformation.

Synthesis of caldarchaeyl-bis-PE as precursor for labeled MSLs with a spacer

The MSPE derivative of a purified caldarchaeol mixture containing mainly from one to three cyclopentane rings with a prevalence of those with two rings was prepared with slight modifications as described for the synthesis of phosphatidylethanolamine (47). As shown in Fig. 3, the reaction proceeded via the caldarchaeo-bis-phosphoric ester dichloride, which in turn was then converted by reaction with ethanolamine into the corresponding bis-oxazaphospholane. This latter intermediate was eventually hydrolyzed in a mixture of THF, acetic acid, water, and methanol to MSPE (Fig. 3), which after chromatographic fractionation resulted in a mixture of MSPE with mainly two cyclopentane rings apart from MSPE with one or three five-membered rings in an overall yield of ~45% starting from caldarchaeol. This moderate yield is due to the fact that in our small-scale preparation traces of water have a significant influence on the moisture-sensitive reaction. Furthermore, caldarchaeol in contrast with diacylglycerol contains two functional hydroxyl groups also resulting in side products such as caldarchaeo-bis-phosphoric acid, phosphoryl-caldarchaeo-phosphoethanolamine, and their corresponding methyl esters. The formation of the methyl esters was due to the presence of methanol, which was added to dissolve the caldarchaeo-bis-oxazaphospholane. The methyl ester formation could be suppressed to some extent by substituting 2-propanol for methanol. It should be emphasized that the condition of phosphorylation of caldarchaeol by phosphoroxychloride has to be correctly chosen to avoid the formation of unwanted side products. Thus, a solution of

caldarchaeol in an inert solvent should be dropped into an excess of phosphoroxychloride, not vice versa, to ensure the formation of a phosphate monoester dichloride rather than a phosphate diester monochloride or, equally worse, a phosphor triester. It was unexpected and surprising to learn that MSPE on TLC moved only half as fast as dioleoyl phosphatidylethanolamine, although the ratio of polar to hydrophobic moiety is nearly the same in both compounds.

Synthesis of caldarchaeyl-bis-amine as precursor for labeled MSLs without a spacer

Because of the restrictions mentioned in the foregoing section, we turned to a different synthetic approach (Fig. 4) to prepare a caldarchaeol derivative that is suited for coupling fluorescent or other label to both ends of the lipid core of caldarchaeol. Therefore, we used well-known synthetic steps that promised more satisfying yields of the final desired products than gained via MSPE. The intermediate we aimed at was a caldarchaeyl-bis-amine, which allowed tying of the label directly to the lipid core with, for instance, the possibility to place a fluorophore closer to a hydrophobic environment when in bilayer membranes, and hence possibly enhancing the quantum yield of fluorescence upon excitation. In this way, the negatively charged phosphoethanolamine spacer could be omitted as well. Fig. 4 depicts a three-step synthetic route to caldarchaeyl-bis-amine from caldarchaeol via the tosylate and the azide. All individual synthetic steps proceeded with yields well above 90%.

Fluorescent membrane-spanning bipolar tetraether lipids

Fluorescently labeled lipids that are resistant to spontaneous as well as protein-mediated intermembrane transfer are necessary for an unambiguous FRET-based membrane fusion and intermembrane lipid transfer assay. As already mentioned in the introduction, the use of bipolar tetraether lipids seems to be well suited for this task. Fig. 5 presents an overview of homosubstituted fluorescent caldarchaeol derivatives described in this article. Fig. 5A shows the structures of NBD-, TAMRA-, and ATTO-MSPE; whereas Fig. 5B displays the structures of NBD- and TAMRA-MSL that do not contain a spacer between the fluorophore and the lipid core. For a comparison of their chromatographic behavior, all five fluorescent MSLs are shown on a TLC plate (Fig. 5C). With the exception of ATTO-MSPE, the fluorescent MSPE derivatives on TLC migrate far less than their respective MSL derivatives owing to their polar phosphoethanolamine part. This polar influence on migration is obviously overcome by the huge lipophilic ATTO residue in ATTO-MSPE. It is conspicuous that both TAMRA-MSL and TAMRA-MSPE clearly separate into a double and triple band, respectively. This can be plausibly explained by the fact that two positional isomers with respect to the carboxyl group of the TAMRA fluorophore were used in the synthesis of these fluorescent lipids. The TAMRA residue may also have an influence on the separation of derivatives with different numbers of five-membered rings as indicated by chromatographic splitting into three bands for TAMRA-MSPE with the middle band of highest intensity. Owing to the high price, we refrained from using the commercially available single isomers. For their use as a quencher for NBD fluorescence, the position of the carboxyl group in this fluorophore is not relevant.

All fluorescent derivatives presented here were obtained by reacting membrane-spanning MSPE and caldarchaeyl-bis-amine with commercially available amine-reactive fluorophores to yield NBD-MSPE, TAMRA-MSPE, and ATTO647N-MSPE, as well as NBD-MSL and TAMRA-MSL, respectively (Fig. 5). In the MSL derivatives, the fluorophore is tied directly to the lipid core via a nitrogen bridge replacing the spacer phosphoethanolamine. Hence, when integrated in lipid bilayers, the fluorophore was expected to be located closer to the hydrophobic layer with concomitant increase in quantum yield of fluorescence than when linked via a phosphoethanolamine spacer. Our measurements, however, did not acknowledge our expectation. A significant increase of NBD fluorescence of NBD-MSL compared with that of NBD-MSPE was not observed. This may be due to the fact that the labeled head group of NBD-MSPE is not stretched away from but tilted to the lipid bilayer as was found for phosphatidylcholine and other amphipathic lipids (59). Thus, for both NBD-MSL and NBD-MSPE, the fluorophore may be equally close to the lipid layer. Nonetheless, the synthesis of the MSL derivatives, in our hands, was much simpler and rewarding with better yields than obtained for MSPE derivatives. On the other hand, spacer linked ligands are required when the ligands have to come within reach of a binding site of proteins such as for instance lectins or enzymes. Therefore, labeling (e.g., with a biotin residue) is usually performed via a spacer to ensure binding to streptavidin. So far we have synthesized a biotinylated MSPE derivative (not shown). This nonextractable lipid can replace extractable biotin-PE in transfer and fusion assays in biotinylated donor liposomes that have to be separated from fluorescent acceptor liposomes by streptavidin-coated magnetic beads (60, 61).

One other simple procedure seems conceivable for the synthesis of spacer-linked ligands, such as for instance fluorophores or carbohydrates. This could make use of a copper(I)-catalyzed azide-alkyne cycloaddition (62, 63) known as click reaction, using caldarchaeyl-bis-azide (Fig. 4) and commercially available ligands, either fluorophores or sugars that contain an alkyne group. Alternatively, because most fluorophores are available with a carboxyl function, these can be converted simply into derivatives with alkyne functionality by reacting with propargylamine to the respective amide prior to the click reaction with caldarchaeyl-bis-azide. In transfer assays that make use of 2-NBD-glycosphingolipids (20), TAMRA-MSPE and TAMRA-MSL proved to be excellent quenchers for NBD fluorescence. In case of excited Rh-PE, a suitable quencher is ATTO-MSPE. NBD-MSPE and TAMRA-MSPE (or TAMRA-MSL) turned out to be a well-suited donor-acceptor pair to study membrane fusion in FRET assays. Likewise, excited TAMRA-MSPE is well quenched by equimolar amounts of ATTO-MSPE and could thus serve as an alternative donor-acceptor pair in membrane fusion studies.

Transfer and fusion assay

A schematic overview of the intermembrane transfer and fusion assay by FRET is depicted in **Fig. 6** (upper panel). The transfer assay is based on fluorescence dequench that occurs when the labeled lipid molecules are transferred from donor membranes to quencher-free acceptor membranes (20). In the study now presented, the donor membranes contain novel and fluorescent bipolar membrane-spanning quencher molecules that are resistant to transfer by proteins. The fusion assay is based on the concentration-dependent changes in fluorescence intensity that occur when donor liposomes containing both nontransferable fluorescent MSLs, such as NBD-MSPE and TAMRA-MSPE that function as a FRET pair, are mixed with nonfluorescent acceptor liposomes. A prerequisite for the fluorescent sphingolipids to act as sensitive transfer probes is their low off-rate (64, 65), which prevents spontaneous transfer between membranes. A low off-rate is a feature of all natural sphingolipids having a long acyl chain in their Cer residue. At present, commercially available fluorescent sphingolipids such as C6-NBD-Cer, -GlcCer, and -lactosylceramide, as well as some BODIPY-labeled sphingolipids, have a high off-rate due to shorter acyl chains with the fluorophore at their methyl end, namely in their omega position. Therefore, these lipids undergo spontaneous intermembrane transfer (66–68). To avoid this drawback in protein-mediated transfer studies, we used fluorescent sphingolipids with a long acyl chain and with the fluorophore in its α or 2 position (20). We chose the NBD group because it is one of the smallest fluorophores. The excitation wavelength of NBD is well separated from its emission wavelength, and the latter overlaps nicely with the excitation wavelength of rhodamine and TAMRA used as quenching fluorophores. From all commercially available amine-reactive fluorophores, NBDF is the most reactive one facilitating efficient and simple labeling (see Materials and Methods). Although the quantum yield and photostability of NBD compared with BODIPY are much less, they are sufficiently sensitive and stable for FRET assays (20, 69). Furthermore, in contrast to BODIPY and other fluorophores, the NBD group is readily reducible by membrane-impermeable dithionite allowing us to test whether liposomes are mono- or multilamellar. When these 2-NBD-sphingolipids are components of bilayer membranes, the NBD group is located at the interface where the lipophilic core meets the aqueous environment, and thus likely causing little, if any, membrane perturbation.

We would like to stress that membrane fusion can be measured easily and accurately by the use of nonextractable MSLs as a fluorescent donor-acceptor pair (FRET pair). If in this fusion assay dequenching is observed, then fusion of membranes must have occurred. On the other hand, a lack of dequenching clearly means that no fusion

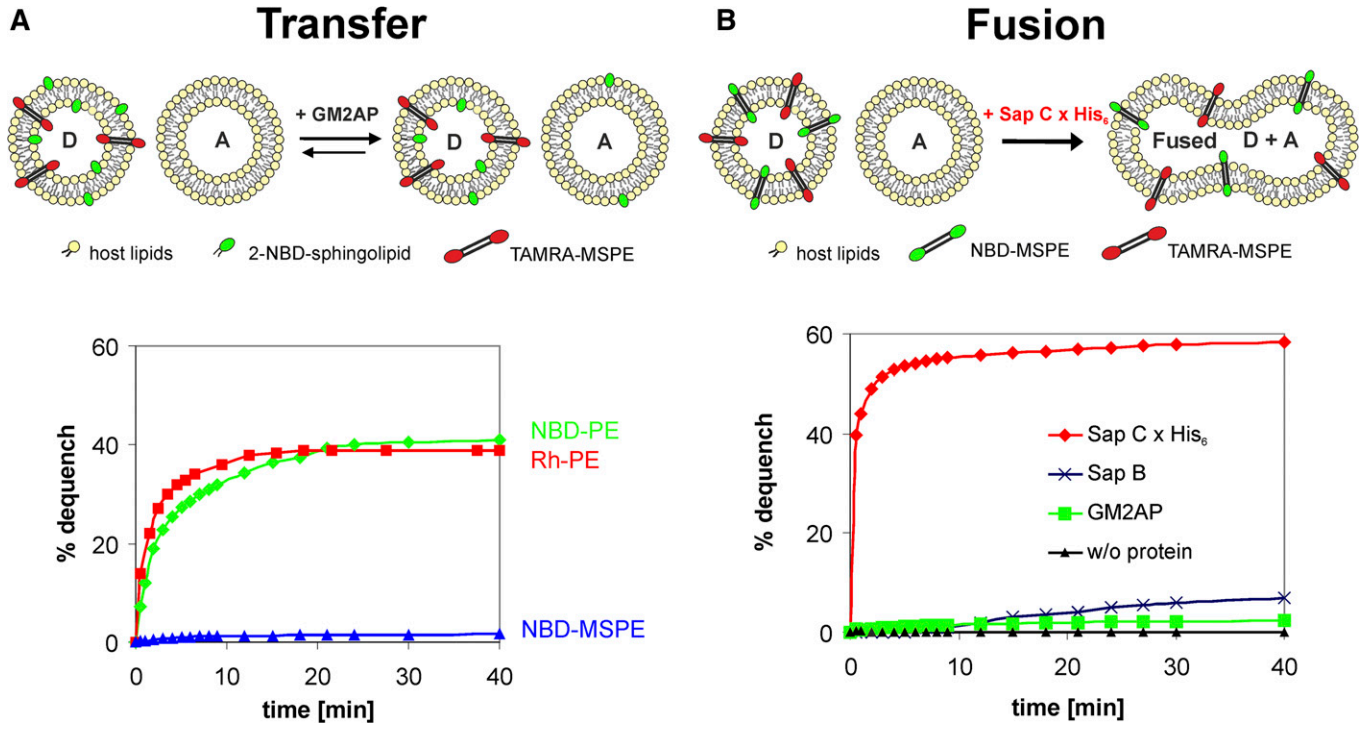

Fig. 6. Intermembrane lipid transfer and membrane fusion assays. A: Upper panel depicts an illustration of a GM2AP-mediated intermembrane transfer process. Lower panel demonstrates that the membrane-spanning NBD-MSPE is almost resistant to extraction by GM2AP, whereas both NBD-PE and Rh-PE are not and are transferred from donor to acceptor liposomes with concomitant dequench of fluorescence. For NBD-PE, the quencher was TAMRA-MSPE, and for Rh-PE, the quencher was ATTO-MSPE. B: Upper panel shows an illustration of a fusion process of donor and acceptor liposomes. Lower panel demonstrates that a recombinant protein with a His-tag (i.e., Sap C x His_6) causes immediate fusion of the vesicles. In the absence of protein, no fusion occurs. A 100% dequench is defined by the fluorescence measured in the absence of quencher. A, acceptor liposome; D, donor liposome. SEM was in the range of 3–5% (n = 3).

has taken place. In the transfer assay, the NBD-labeled MSL is replaced by a 2-NBD-sphingolipid. Provided that fusion has been excluded in the fusion assay, any fluorescence dequench proves 2-NBD-lipid transfer. If no dequench is measured, then neither membrane fusion nor lipid transfer has occurred. If, in both assays, dequench is observed, then the protein under study may have induced both membrane fusion and intermembrane lipid transfer. However, if fusion is fast and outweighs transfer, the latter becomes meaningless. This is also true for the opposite. In cases, should they occur, where protein-mediated membrane fusion and intermembrane lipid transfer are of comparable rate, no distinction between the two can be made. In this special case, there is, to the best of our knowledge, no method available to distinguish protein-mediated membrane fusion from lipid transfer.

A combined use of TAMRA-MSPE and ATTO-MSPE in the same donor vesicles could serve for a concomitant measurement of intermembrane lipid transfer and membrane fusion to address the question of whether one and the same protein transfers lipids and/or fuses vesicles simultaneously. This kind of assay may be of importance if the protein or lipid under study is scarce. Naturally, this test requires an alternating setting of the excitation and emission wavelength.

We addressed the question of whether the bipolar membrane-spanning quencher molecules would influence the extractability of sphingolipids by SAPs. As shown in **Fig. 7A**, no significant influence on intermembrane transfer of 2-NBD-sulfatide by GM2AP could be observed even if the concentration of TAMRA-MSPE was increased 4-fold and well above the concentration needed for quenching of the NBD fluorescence.

GM2AP mediates intermembrane transfer of phosphoglycerides but not of MSLs

As proof of principle, we studied whether NBD-MSPE is pulled out of lipid bilayers by GM2AP or remains stably inserted in membranes. Therefore, we checked by a FRET assay as outlined in an illustration in Fig. 6A (upper panel) whether GM2AP would extract and transfer bipolar NBD-MSPE from and to liposomal membranes. This was not to be expected unless NBD-MSPE would adapt a U-shaped conformation in membranes. Fig. 6A (lower panel) clearly demonstrates that in stark contrast to the phosphoglycerolipids NBD-PE and Rh-PE, the membrane-spanning NBD-MSPE remains almost exclusively in the donor liposome membrane indicating that this compound like BSC stretches across the entire bilayer. Because a small dequench of NBD-MSPE (~2% after 40 min) was observed, a tiny, albeit unlikely, fusogenic property of GM2AP cannot be totally ruled out. Another reason for this little dequench may be that some fusogenic contaminants were copurified with GM2AP. However, it seems more likely that some lipid aggregates other than bilayers were also formed during liposome preparation and slowly merged with the 5-fold excess of acceptor liposomes, thus yielding the observed small dequench. This would also agree with our results obtained upon neuraminidase treatment of BSC (see "Demonstration that caldarchaeol derivatives are membrane spanning"). Under our experimental conditions, the fluorescence of excited NBD-PE as well as Rh-PE was almost totally quenched by membrane-spanning TAMRA-MSPE and ATTO-MSPE, respectively, residing in the same donor liposomes. Upon GM2AP-mediated transfer of the former to acceptor liposomes, which contained no quencher, the fluorescence increased with time and came to equilibrium at ~40% dequench. This value nicely agrees with the theoretical value of ~43% that is reached by equilibrium when the transferable fluorescent lipids of the outer layer of donor liposomes distribute to a 5-fold amount of quencher-free acceptor liposomes. In this case, five-sixths of the available lipids are unquenched, whereas one-sixth yet resides in the donor liposome still being quenched by either TAMRA-MSPE or ATTO-MSPE, respectively (Fig. 6A).

Recombinant Sap C x His_6 causes membrane fusion

Next, we tested the suitability of the FRET pair NBD-MSPE/TAMRA-MSPE in membrane fusion studies as outlined in Fig. 6B (upper panel). When this membrane-spanning FRET pair is present in donor liposomes at an equimolar concentration between 1 and 2 mol%, the emission of excited NBD-MSPE is almost totally quenched by TAMRA-MSPE. However, when membrane fusion was initiated by the addition of a recombinant Sap C x His_6 to 1.5 μM concentration, and in the presence of a 5-fold amount of unlabeled liposomes, an immediate dequench of the NBD fluorescence could be observed (Fig. 6B, lower panel). This rapid fusion process was claimed to be independent of the His-tag or that the His-tag had only a minor impact on membrane fusion, if any (70). In a FRET assay, it was previously shown that Sap C isolated from spleens of patients with Gaucher's disease type 1 induced vesicle fusion (71). These results may have been compromised in as much as the possibility that Sap C, besides initiating fusion, may also have transferred NBD-PE and Rh-PE to acceptor vesicles was not excluded. If this transfer had occurred, then membrane concentration of these reporter lipids would have declined with concomitant increase in NBD fluorescence. In the absence of protein, we observed no dequench in our fusion assay, which indicated that no dilution of the membrane concentration of the labeled reporter molecules by spontaneous vesicle fusion with simultaneous attenuation of FRET had occurred. Some dequench was, however, seen for 2.5 μM Sap B and very little for 0.25 μM GM2AP implying that these proteins might either have some fusogenic property themselves or contain small amounts of fusion proteins (e.g., Sap C coisolated in their purification process). These observations have little bearing on the functioning of this fusion assay though. However, care must be taken when lipid transfer and fusion properties of those recombinant proteins are studied that are expressed with a His-tag and that had not been removed prior to measurements (8).

Both GM2AP and Sap B are promiscuous with respect to sphingolipid transfer

In previous publications, it was shown that GM2AP binds to gangliosides, and among those tested, GM2AP would

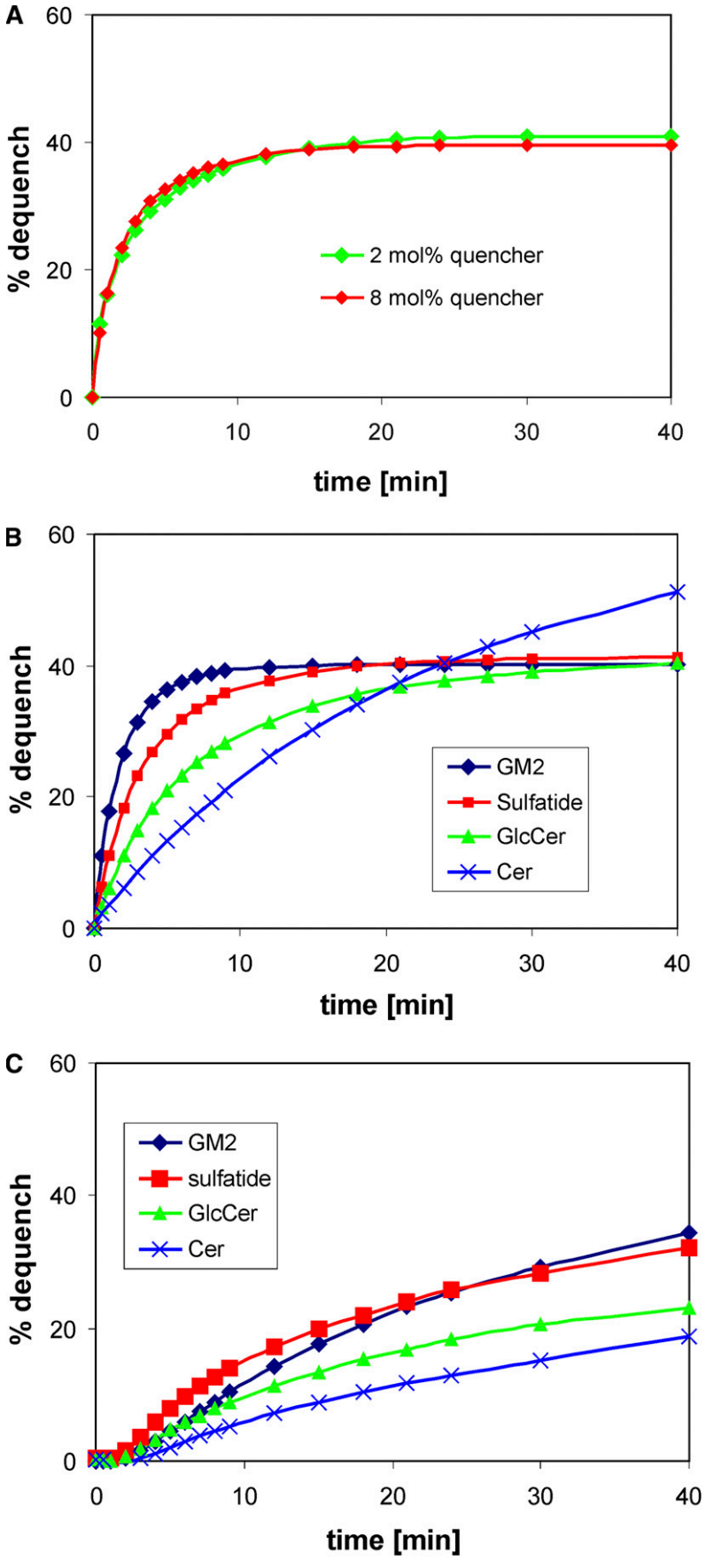

Fig. 7. Intermembrane sphingolipid transfer evoked by 0.2 μM GM2AP (A, B) and by 2.0 μM Sap B (C). The sphingolipids listed in the figure are the respective fluorescent NBD derivatives with the NBD-amino group in the α position of their acyl chain (20). A: The transfer of 2-NBD-sulfatide from donor to acceptor membranes by GM2AP. In this experiment, donor liposomes contained either 2 mol% or 8 mol% TAMRA-MSPE as quencher. Donor liposomes in intermembrane transfer assays of 2-NBD-sphingolipids contained 2 mol% quencher (B, C). All assays were carried out in quadruplicate, and the results agreed within 5%.

bind and transfer more or less avidly gangliosides GM1 and GM2 and to a lesser extent ganglioside GM3, the product of GM2AP-assisted hydrolysis of GM2 by β-hexosaminidase A (32). More recently, it was reported that GM2AP, in addition to these gangliosides, also binds and transfers some phosphoglycerides (22, 72). Thus, for us it became of considerable interest to study the transfer properties of activator proteins with our newly designed FRET assay using sphingolipids with the NBD label in the α position of their long acyl chain such as those described previously (20). To this end, we examined GM2AP and Sap B both of which were available to us in a fairly pure state. As demonstrated in Fig. 7B, all sphingolipids tested were transferred by GM2AP in a hyperbolic fashion albeit with different kinetics. It is conspicuous that the more polar and acidic lipids GM2 and sulfatide are transferred much faster than less polar lipids like GlcCer and Cer. The dequenching of NBD fluorescence of GM2, sulfatide, and GlcCer, with the exception of Cer, came close to the theoretical value (see "GM2AP mediates intermembrane transfer of phosphoglycerides but not of MSLs"). The fluorescence of Cer surpassed the value of 43% and approached >50% already after 40 min with no sign of reaching a plateau. Even though slowly transferred, the dequenching of NBD fluorescence of 2-NBD-Cer reached a plateau at ~83% after 90 min (data not shown). This phenomenon is plausibly explained by assuming that Cer, having no polar head group such as sugars or phosphoryl choline, undergoes a transversal diffusion (flip-flop) in lipid bilayers and thus becomes accessible to lipid binding and transfer proteins. This finding was corroborated by a complete loss of the NBD fluorescence of liposomal 2-NBD-Cer by reduction with dithionite. Transbilayer movement in cellular membranes of short acyl chain NBD-Cers [e.g., NBD-C6-Cer and its *O*-methyl ether (73)] and of a BODIPY-labeled Cer in phospholipid bilayers (66) has been observed before. On the other hand, dithionite reduced only ~50% of 2-NBD-glycosphingolipid fluorescence (data not shown), for these lipids with a polar head group are not prone to transversal diffusion without the help of a flippase.

Fig. 7C shows that Sap B is also active in intermembrane lipid transfer. Again, the rate of transfer seems to depend on the polarity of the sphingolipid and agrees with the observation made in an earlier study (74). Here, we found transfer of sulfatide a little faster than transfer of GM2. It may be speculated that Sap B prefers sulfatide over other sphingolipids for it is a factor sine qua non in lysosomal sulfatide degradation. It is interesting to note that sphingolipid transfer evoked by Sap B follows sigmoidal kinetics rather than hyperbolic kinetics and is much slower than that catalyzed by GM2AP, even though a 10-fold higher protein concentration was used. The reason for this phenomenon can only be speculated on. Previous crystallographic analysis disclosed the structure of unglycosylated Sap B as a shell-like homodimer, enclosing a large hydrophobic cavity (75). Based on the structure and on binding studies with lipids, the following hypothetical mechanism for the interaction of Sap B with membranes was proposed (75). In the open conformation, the homodimer interacts directly with the membrane. After extraction of a lipid substrate, it changes into a closed conformation. Thus, Sap B may function as a lipid binding and transfer protein of broad specificity (74) when in the correct conformational state. Because Sap B in solution tends to aggregate to oligomers, it may take some time for these aggregates to rearrange into the active conformation at the liposomal surface before lipid binding and extraction can occur. This may give rise to the initial sigmoidal shape of the dequenching curve seen in Fig. 7C.

CONCLUSION AND PROSPECTS

This work addressed the use of membrane-spanning fluorescent lipids in FRET assays and their importance for studying protein-mediated intermembrane lipid transfer as well as membrane fusion. These novel nonextractable reporter molecules allow for the first time unambiguous measurements of these processes, which are necessary to shed light on the activity of the activator proteins in the lysosomal degradation of sphingolipids and in intraendosomal/intralysosomal membrane disintegration. The findings reported in this study demonstrate that our newly developed FRET assay is well suited to study in real time intermembrane lipid transfer and/or membrane fusion caused by lysosomal lipid binding proteins. In addition, the nonextractable membrane-spanning reporter molecules may also be helpful in the study of the selectivity and requirements of other LTPs. These LTPs are ubiquitous in the cytoplasm of eukaryotic cells and are involved, for instance, in intermembrane transfer of oxysterol and phospholipids (76–79), as well as Cer derivatives and glycolipids (1, 64, 80, 81). Furthermore, these FRET assays allow us to study in real time, without the need to separate vesicles, and in more detail the activities of activator proteins and their variant forms. The data obtained indicate that the rapid and robust system presented here should serve as a valuable tool to probe quantitatively and comprehensively the membrane activity of GM2AP and other SAPs and facilitate further structure-function studies aimed at delineating independently the lipid- and the enzyme-binding mode of these essential cofactors. The radioactive and glycosylated caldarchaeol derivatives may help in delineating the kinetics of membrane disintegration in the hydrolytic compartments of living cells and may be of advantage in disclosing more of the functions of lysosomal activator proteins.

The authors thank Jennifer Mainzer, Heike Hupfer, and Christine Beuss for technical assistance.

REFERENCES

1. Brown, R. E., and P. Mattjus. 2007. Glycolipid transfer proteins. *Biochim. Biophys. Acta.* **1771:** 746–760.
2. Schuette, C. G., B. Pierstorff, S. Huettler, and K. Sandhoff. 2001. Sphingolipid activator proteins: proteins with complex functions in lipid degradation and skin biogenesis. *Glycobiology.* **11:** 81R–90R.
3. Schulze, H., T. Kolter, and K. Sandhoff. 2009. Principles of lysosomal membrane degradation: Cellular topology and biochemistry of lysosomal lipid degradation. *Biochim. Biophys. Acta.* **1793:** 674–683.

4. Wilkening, G., T. Linke, G. Uhlhorn-Dierks, and K. Sandhoff. 2000. Degradation of membrane-bound ganglioside GM1. Stimulation by bis(monoacylglycero)phosphate and the activator proteins SAP-B and GM2-AP. *J. Biol. Chem.* **275:** 35814–35819.
5. Conzelmann, E., and K. Sandhoff. 1979. Purification and characterization of an activator protein for the degradation of glycolipids GM2 and GA2 by hexosaminidase A. *Hoppe Seylers Z. Physiol. Chem.* **360:** 1837–1849.
6. Hechtman, P. 1977. Characterization of an activating factor required for hydrolysis of Gm2 ganglioside catalyzed by hexosaminidase A. *Can. J. Biochem.* **55:** 315–324.
7. Conzelmann, E., and K. Sandhoff. 1978. AB variant of infantile GM2 gangliosidosis: deficiency of a factor necessary for stimulation of hexosaminidase A-catalyzed degradation of ganglioside GM2 and glycolipid GA2. *Proc. Natl. Acad. Sci. USA.* **75:** 3979–3983.
8. Anheuser, S., B. Breiden, G. Schwarzmann, and K. Sandhoff. 2015. Membrane lipids regulate ganglioside GM2 catabolism and GM2 activator protein activity. *J. Lipid Res.* Epub ahead of print. July 14, 2015; doi:10.1194/jlr.M061036.
9. Harzer, K., B. C. Paton, H. Christomanou, M. Chatelut, T. Levade, M. Hiraiwa, and J. S. O'Brien. 1997. Saposins (sap) A and C activate the degradation of galactosylceramide in living cells. *FEBS Lett.* **417:** 270–274.
10. Fischer, G., and H. Jatzkewitz. 1975. The activator of cerebroside sulphatase. Purification from human liver and identification as a protein. *Hoppe Seylers Z. Physiol. Chem.* **356:** 605–613.
11. Christomanou, H., A. Aignesberger, and R. P. Linke. 1986. Immunochemical characterization of two activator proteins stimulating enzymic sphingomyelin degradation in vitro. Absence of one of them in a human Gaucher disease variant. *Biol. Chem. Hoppe Seyler.* **367:** 879–890.
12. Wilkening, G., T. Linke, and K. Sandhoff. 1998. Lysosomal degradation on vesicular membrane surfaces. Enhanced glucosylceramide degradation by lysosomal anionic lipids and activators. *J. Biol. Chem.* **273:** 30271–30278.
13. Berent, S. L., and N. S. Radin. 1981. Mechanism of activation of glucocerebrosidase by co-beta-glucosidase (glucosidase activator protein). *Biochim. Biophys. Acta.* **664:** 572–582.
14. Linke, T., G. Wilkening, F. Sadeghlar, H. Mozcall, K. Bernardo, E. Schuchman, and K. Sandhoff. 2001. Interfacial regulation of acid ceramidase activity. Stimulation of ceramide degradation by lysosomal lipids and sphingolipid activator proteins. *J. Biol. Chem.* **276:** 5760–5768.
15. Harzer, K., B. C. Paton, A. Poulos, B. Kustermann-Kuhn, W. Roggendorf, T. Grisar, and M. Popp. 1989. Sphingolipid activator protein deficiency in a 16-week-old atypical Gaucher disease patient and his fetal sibling: biochemical signs of combined sphingolipidoses. *Eur. J. Pediatr.* **149:** 31–39.
16. Salio, M., H. Ghadbane, O. Dushek, D. Shepherd, J. Cypen, U. Gileadi, M. C. Aichinger, G. Napolitani, X. Qi, P. A. van der Merwe, et al. 2013. Saposins modulate human invariant natural killer T cells self-reactivity and facilitate lipid exchange with CD1d molecules during antigen presentation. *Proc. Natl. Acad. Sci. USA.* **110:** E4753–E4761.
17. Winau, F., V. Schwierzeck, R. Hurwitz, N. Remmel, P. A. Sieling, R. L. Modlin, S. A. Porcelli, V. Brinkmann, M. Sugita, K. Sandhoff, et al. 2004. Saposin C is required for lipid presentation by human CD1b. *Nat. Immunol.* **5:** 169–174.
18. Förster, T. 1949. Experimentelle und theoretische Untersuchung des zwischenmolekularen Übergangs von Elektronenanregungsenergie. *Z. Naturforsch. A.* **4:** 321–327.
19. Struck, D. K., D. Hoekstra, and R. E. Pagano. 1981. Use of resonance energy transfer to monitor membrane fusion. *Biochemistry.* **20:** 4093–4099.
20. Schwarzmann, G., M. Wendeler, and K. Sandhoff. 2005. Synthesis of novel NBD-GM1 and NBD-GM2 for the transfer activity of GM2-activator protein by a FRET-based assay system. *Glycobiology.* **15:** 1302–1311.
21. Wendeler, M., N. Werth, T. Maier, G. Schwarzmann, T. Kolter, M. Schoeniger, D. Hoffmann, T. Lemm, W. Saenger, and K. Sandhoff. 2006. The enzyme-binding region of human GM2-activator protein. *FEBS J.* **273:** 982–991.
22. Ran, Y., and G. E. Fanucci. 2009. Ligand extraction properties of the GM2 activator protein and its interactions with lipid vesicles. *Biophys. J.* **97:** 257–266.
23. Beveridge, T. J., C. G. Choquet, G. B. Patel, and G. D. Sprott. 1993. Freeze-fracture planes of methanogen membranes correlate with the content of tetraether lipids. *J. Bacteriol.* **175:** 1191–1197.
24. De Rosa, M., A. Gambacorta, and A. Gliozzi. 1986. Structure, biosynthesis, and physicochemical properties of archaebacterial lipids. *Microbiol. Rev.* **50:** 70–80.
25. Elferink, M. G., J. G. de Wit, R. Demel, A. J. Driessen, and W. N. Konings. 1992. Functional reconstitution of membrane proteins in monolayer liposomes from bipolar lipids of Sulfolobus acidocaldarius. *J. Biol. Chem.* **267:** 1375–1381.
26. Gliozzi, A., R. Rolandi, M. De Rosa, A. Gambacorta, and B. Nicolaus. 1982. Membrane models of archaebacteria. *In* Transport in Biomembranes: Model Systems and Reconstitution. R. Antolini, editor. Raven Press, New York. 39–47.
27. Langworthy, T. A. 1978. Membranes and lipids of extremely thermoacidophilic microorganisms. *In* Biochemistry of Thermophily. S. M. Friedman, editor. Academic Press, New York. 11–30.
28. Gliozzi, A., M. Robello, A. Relini, and G. Accardo. 1994. Asymmetric black membranes formed by one monolayer of bipolar lipids at the air/water interface. *Biochim. Biophys. Acta.* **1189:** 96–100.
29. Gliozzi, A., R. Rolandi, M. De Rosa, and A. Gambacorta. 1982. Artificial black membranes from bipolar lipids of thermophilic archaebacteria. *Biophys. J.* **37:** 563–566.
30. Gliozzi, A., R. Rolandi, M. De Rosa, and A. Gambacorta. 1983. Monolayer black membranes from bipolar lipids of archaebacteria and their temperature-induced structural-changes. *J. Membr. Biol.* **75:** 45–56.
31. Cuccia, L. A., F. Morin, A. Beck, N. Hébert, G. Just, and R. B. Lennox. 2000. Spanning or looping? The order and conformation of bipolar phospholipids in lipid membranes using 2H NMR spectroscopy. *Chemistry.* **6:** 4379–4384.
32. Conzelmann, E., J. Burg, G. Stephan, and K. Sandhoff. 1982. Complexing of glycolipids and their transfer between membranes by the activator protein for degradation of lysosomal ganglioside GM2. *Eur. J. Biochem.* **123:** 455–464.
33. Meier, E. M., G. Schwarzmann, W. Fürst, and K. Sandhoff. 1991. The human GM2 activator protein. A substrate specific cofactor of beta-hexosaminidase A. *J. Biol. Chem.* **266:** 1879–1887.
34. Smiljanic-Georgijev, N., B. Rigat, B. Xie, W. Wang, and D. J. Mahuran. 1997. Characterization of the affinity of the G(M2) activator protein for glycolipids by a fluorescence dequenching assay. *Biochim. Biophys. Acta.* **1339:** 192–202.
35. Schwarzmann, G., C. Arenz, and K. Sandhoff. 2014. Labeled chemical biology tools for investigating sphingolipid metabolism, trafficking and interaction with lipids and proteins. *Biochim. Biophys. Acta.* **1841:** 1161–1173.
36. Yasuda, M., H. Oyaizu, A. Yamagishi, and T. Oshima. 1995. Morphological variation of new Thermoplasma acidophilum isolates from Japanese hot springs. *Appl. Environ. Microbiol.* **61:** 3482–3485.
37. Uda, I., A. Sugai, Y. H. Itoh, and T. Itoh. 2001. Variation in molecular species of polar lipids from Thermoplasma acidophilum depends on growth temperature. *Lipids.* **36:** 103–105.
38. Gräther, O., and D. Arigoni. 1995. Detection of regioisomeric macrocyclic tetraethers in the lipids of Methanobacterium thermoautotrophicum and other archaeal organisms. *J Chem Soc Chem Comm.* **4:** 405–406.
39. Koga, Y., and H. Morii. 2005. Recent advances in structural research on ether lipids from archaea including comparative and physiological aspects. *Biosci. Biotechnol. Biochem.* **69:** 2019–2034.
40. Heathcock, C. H., B. L. Finkelstein, E. T. Jarvi, P. A. Radel, and C. R. Hadley. 1988. Acyclic stereoselection. Part 42. 1,4- and 1,5-Stereoselection by sequential aldol addition to alpha,beta-unsaturated aldehydes followed by Claisen rearrangement. Application to total synthesis of the vitamin E side chain and the archaebacterial C40 diol. *J. Org. Chem.* **53:** 1922–1942.
41. Montenegro, E., B. Gabler, G. Paradies, M. Seemann, and G. Helmchen. 2003. Determination of the configuration of an archaea membrane lipid containing cyclopentane rings by total synthesis. *Angew. Chem. Int. Ed. Engl.* **42:** 2419–2421.
42. Dess, D. B., and J. C. Martin. 1983. Readily accessible 12-I-5 oxidant for the conversion of primary and secondary alcohols to aldehydes and ketones. *J. Org. Chem.* **48:** 4155–4156.
43. Schwarzmann, G., P. Hofmann, and U. Pütz. 1997. Synthesis of ganglioside GM1 containing a thioglycosidic bond to its labeled ceramide(s). A facile synthesis starting from natural gangliosides. *Carbohydr. Res.* **304:** 43–52.
44. Koenigs, W., and E. Knorr. 1901. Ueber einige Derivate des Traubenzuckers und der Galactose. *Ber Dtsch Chem Ges.* **34:** 957–981.
45. Helferich, B., and K. Weis. 1956. Zur Synthese von Glucosiden und von nicht-reduzierenden Disacchariden. *Chem. Ber.* **89:** 314–321.

46. Schwarzmann, G., and K. Sandhoff. 1987. Lysogangliosides: synthesis and use in preparing labeled gangliosides. *Methods Enzymol.* **138:** 319–341.
47. Eibl, H. 1978. Phospholipid synthesis: oxazaphospholanes and dioxaphospholanes as intermediates. *Proc. Natl. Acad. Sci. USA.* **75:** 4074–4077.
48. Folch, J., M. Lees, and G. H. Sloane Stanley. 1957. A simple method for the isolation and purification of total lipides from animal tissues. *J. Biol. Chem.* **226:** 497–509.
49. Kobayashi, T., M. H. Beuchat, M. Lindsay, S. Frias, R. D. Palmiter, H. Sakuraba, R. G. Parton, and J. Gruenberg. 1999. Late endosomal membranes rich in lysobisphosphatidic acid regulate cholesterol transport. *Nat. Cell Biol.* **1:** 113–118.
50. Möbius, W., E. van Donselaar, Y. Ohno-Iwashita, Y. Shimada, H. F. Heijnen, J. W. Slot, and H. J. Geuze. 2003. Recycling compartments and the internal vesicles of multivesicular bodies harbor most of the cholesterol found in the endocytic pathway. *Traffic.* **4:** 222–231.
51. Bierfreund, U., T. Kolter, and K. Sandhoff. 2000. Sphingolipid hydrolases and activator proteins. *Methods Enzymol.* **311:** 255–276.
52. Sandhoff, K., K. Harzer, W. Wassle, and H. Jatzkewitz. 1971. Enzyme alterations and lipid storage in three variants of Tay-Sachs disease. *J. Neurochem.* **18:** 2469–2489.
53. Fahy, E., S. Subramaniam, H. A. Brown, C. K. Glass, A. H. Merrill, Jr., R. C. Murphy, C. R. Raetz, D. W. Russell, Y. Seyama, W. Shaw, et al. 2005. A comprehensive classification system for lipids. *J. Lipid Res.* **46:** 839–861.
54. Shimada, H., N. Nemoto, Y. Shida, T. Oshima, and A. Yamagishi. 2002. Complete polar lipid composition of Thermoplasma acidophilum HO-62 determined by high-performance liquid chromatography with evaporative light-scattering detection. *J. Bacteriol.* **184:** 556–563.
55. Eguchi, T., K. Ibaragi, and K. Kakinuma. 1998. Total synthesis of archaeal 72-membered macrocyclic tetraether lipids. *J. Org. Chem.* **63:** 2689–2698.
56. Mraz, W., G. Schwarzmann, J. Sattler, T. Momoi, B. Seemann, and H. Wiegandt. 1980. Aggregate formation of gangliosides at low concentrations in aqueous media. *Hoppe Seylers Z. Physiol. Chem.* **361:** 177–185.
57. Whiles, J. A., R. Deems, R. R. Vold, and E. A. Dennis. 2002. Bicelles in structure-function studies of membrane-associated proteins. *Bioorg. Chem.* **30:** 431–442.
58. McIntyre, J. C., and R. G. Sleight. 1991. Fluorescence assay for phospholipid membrane asymmetry. *Biochemistry.* **30:** 11819–11827.
59. Brown, M. F., and J. Seelig. 1977. Ion-induced changes in head group conformation of lecithin bilayers. *Nature.* **269:** 721–723.
60. Babalola, J. O., M. Wendeler, B. Breiden, C. Arenz, G. Schwarzmann, S. Locatelli-Hoops, and K. Sandhoff. 2007. Development of an assay for the intermembrane transfer of cholesterol by Niemann-Pick C2 protein. *Biol. Chem.* **388:** 617–626.
61. Abdul-Hammed, M., B. Breiden, M. A. Adebayo, J. O. Babalola, G. Schwarzmann, and K. Sandhoff. 2010. Role of endosomal membrane lipids and NPC2 in cholesterol transfer and membrane fusion. *J. Lipid Res.* **51:** 1747–1760.
62. Huisgen, R. 1961. 1,3-Dipolar cycloadditions. *Proc Chem Soc London.* **1961:** 357–369.
63. Kolb, H. C., M. G. Finn, and K. B. Sharpless. 2001. Click chemistry: diverse chemical function from a few good reactions. *Angew. Chem. Int. Ed. Engl.* **40:** 2004–2021.
64. Brown, R. E., F. A. Stephenson, T. Markello, Y. Barenholz, and T. E. Thompson. 1985. Properties of a specific glycolipid transfer protein from bovine brain. *Chem. Phys. Lipids.* **38:** 79–93.
65. Roseman, M. A., and T. E. Thompson. 1980. Mechanism of the spontaneous transfer of phospholipids between bilayers. *Biochemistry.* **19:** 439–444.
66. Bai, J., and R. E. Pagano. 1997. Measurement of spontaneous transfer and transbilayer movement of BODIPY-labeled lipids in lipid vesicles. *Biochemistry.* **36:** 8840–8848.
67. Nichols, J. W., and R. E. Pagano. 1981. Kinetics of soluble lipid monomer diffusion between vesicles. *Biochemistry.* **20:** 2783–2789.
68. Nichols, J. W., and R. E. Pagano. 1982. Use of resonance energy transfer to study the kinetics of amphiphile transfer between vesicles. *Biochemistry.* **21:** 1720–1726.
69. Haldar, S., and A. Chattopadhyay. 2013. Application of NBD-labeled lipids in membrane and cell biology. *In* Fluorescent Methods to Study Biological Membranes. Y. Mély and G. Duportail, editors. Springer, Berlin. 37–50.
70. Qi, X., and Z. Chu. 2004. Fusogenic domain and lysines in saposin C. *Arch. Biochem. Biophys.* **424:** 210–218.
71. Vaccaro, A. M., M. Tatti, F. Ciaffoni, R. Salvioli, A. Serafino, and A. Barca. 1994. Saposin C induces pH-dependent destabilization and fusion of phosphatidylserine-containing vesicles. *FEBS Lett.* **349:** 181–186.
72. Ran, Y., and G. E. Fanucci. 2008. A dansyl fluorescence-based assay for monitoring kinetics of lipid extraction and transfer. *Anal. Biochem.* **382:** 132–134.
73. Pütz, U., and G. Schwarzmann. 1995. Golgi staining by two fluorescent ceramide analogues in cultured fibroblasts requires metabolism. *Eur. J. Cell Biol.* **68:** 113–121.
74. Vogel, A., G. Schwarzmann, and K. Sandhoff. 1991. Glycosphingolipid specificity of the human sulfatide activator protein. *Eur. J. Biochem.* **200:** 591–597.
75. Ahn, V. E., K. F. Faull, J. P. Whitelegge, A. L. Fluharty, and G. G. Prive. 2003. Crystal structure of saposin B reveals a dimeric shell for lipid binding. *Proc. Natl. Acad. Sci. USA.* **100:** 38–43.
76. Lev, S. 2012. Nonvesicular lipid transfer from the endoplasmic reticulum. *Cold Spring Harb. Perspect. Biol.* **4:** a013300.
77. Mesmin, B., J. Bigay, J. Moser von Filseck, S. Lacas-Gervais, G. Drin, and B. Antonny. 2013. A four-step cycle driven by PI(4)P hydrolysis directs sterol/PI(4)P exchange by the ER-Golgi tether OSBP. *Cell.* **155:** 830–843.
78. Simanshu, D. K., R. K. Kamlekar, D. S. Wijesinghe, X. Zou, X. Zhai, S. K. Mishra, J. G. Molotkovsky, L. Malinina, E. H. Hinchcliffe, C. E. Chalfant, et al. 2013. Non-vesicular trafficking by a ceramide-1-phosphate transfer protein regulates eicosanoids. *Nature.* **500:** 463–467.
79. Weber-Boyvat, M., W. Zhong, D. Yan, and V. M. Olkkonen. 2013. Oxysterol-binding proteins: functions in cell regulation beyond lipid metabolism. *Biochem. Pharmacol.* **86:** 89–95.
80. Tuuf, J., and P. Mattjus. 2014. Membranes and mammalian glycolipid transferring proteins. *Chem. Phys. Lipids.* **178:** 27–37.
81. Yamaji, T., and K. Hanada. 2015. Sphingolipid metabolism and interorganellar transport: localization of sphingolipid enzymes and lipid transfer proteins. *Traffic.* **16:** 101–122.